



Sudan University of Science and Technology
College Of Graduate Studies



Characterization of Corpus Callosum in Sudanese Population using Magnetic Resonance Imaging

توصيف الجسم الثفني لدى السودانيين باستخدام التصوير بالرنين المغناطيسي

A Research Submitted for Partial Fulfillment of the Requirements of M.Sc.
in Diagnostic Radiography

By:

OMER IBRAHIM OMER HASSAN

Supervisor:

Dr. CAROLIN EDWARD

June 2016

الآية

قال تعالى:

{ إِقْرَأْ بِاسْمِ رَبِّكَ الَّذِي خَلَقَ (1) خَلَقَ الْإِنْسَانَ مِنْ عَلَقٍ
(2) إِقْرَأْ وَرَبُّكَ الْأَكْرَمُ (3) الَّذِي عَلَّمَ بِالْقَلَمِ (4) عَلَّمَ
الْإِنْسَانَ مَا لَمْ يَعْلَمْ (5) }

صدق الله العظيم

سورة العلق الآيات (1-5)

Abstract:

Corpus callosum is vital part of the human brain because it enhances and maintains communication between brain hemispheres. It is likely to be affected by the physiologic, as well as pathological changes occurred in the regions of brain. Also corpus callosum dimensions and texture might be change in respect to age which generally might insinuate or simulate pathology. Therefore Study of normal measurements of corpus callosum is helpful in providing baseline data for recognizing and diagnosing the presence and progression of diseases as well as to differentiate between degenerative changes and pathological changes.

The aim of this work was to provide a Sudanese index (dimension) for corpus callosum and the associated parts in the normal people and the changes in the measurement that attributed to ageing and compare it with the published data.

A number of MRI scans of 50 adult patients (male and female) aged between 10 – 74 years, having no brain disorders that affect the corpus callosum, were collected from department of radiology at Modern Medical Center Al-zaytouna Hospital, and Royal Care International Hospital.

The results showed that the average genu, trunk and selenium widths are 11.63 +/- 1.77, 6.04+/- 1.18 and 11.37 +/- 1.85 mm respectively.

The study concluded that according to the normal cells adaptation the age have direct effect on the corpus callosum size and noted that increase in age lead to decrease in corpus callosum dimensions

مستخلص البحث:

الجسم الثفني بالدماغ تمثل الجزء الحيوى منه ومن المرجح ان تتاثر بالتغيرات الفزيولوجيه و المرضيه فى اجزاء الدماغ ومع تغير عمر الانسان قد يتغير حجم وشكل الجسم الثفني مما قد يحاكي وجود حاله مرضيه بالدماغ.ولهذا دراسة الابعاد الطبيعيه للجسم الثفني مفيد لعمل قاعدة بيانات لتميزوتشخيص وجود وحدة الامراض وايضاً للتفريق بين التغيرات الطبيعيه الناتجه عن تغير العمر (التنكسيه) وبين التغيرات المرضيه. الهدف من هذا العمل توفير فهرس سودانى لابعاد الجسم الثفني ولاجزاء الدماغ المرتبطه به عند الاشخاص غير المصابين بمرض فيه وقياس التغيرات فى ابعاد الجسم الثفني تبعاً للزياده فى العمر ومقارنتها مع البيانات (الدراسات) التى تم نشرها.

تم جمع عدد 50 فحص رنين مغنطيسى للدماغ لمرضى (ذكور واناث) تتراوح اعمارهم ما بين 10 الى 74 ولا يعانون من اى امراض قد تؤثر على الجسم الثفني وتم جمع هذه الفحوصات بقسم الاشعه بكل من المركز الطبى الحديث ومستشفى الزيتونه التخصصي ومستشفى رويال كير العالمى بالسودان.

اظهرت النتائج ان متوسط عرض ركبة وجزع وشريط الجسم الثفني هو 11.36 +/- 1.77 , 6.04 +/- 1.18 , 11.37 +/- 1.85 ملم على التوالي.

وخلصت الدراسه بانه تبعاً للتكيف الطبيعى للخلايا فأن العمر له تأثير مباشر على حجم الجسم الثفني داخل الدماغ وقد لوحظ ان التقدم فى العمر يؤدى الى نقصان ابعاد الجسم الثفني.

Dedication

To my family

To my friends

To my teachers

...

Acknowledgment

First of all, I Thank Allah the almighty for helping me to complete this project. I Thank Dr. CAROLIN EDWARD my supervisor for her help and guidance .finally I would like to thank everybody who helped me in this project.

List of contents:

Topic	Page
الإليه	I
Abstract English	II
Abstract Arabic	III
Dedication	IV
Acknowledgment	V
List of content	VI-VII
List of figures	VIII
List of tables	XI
Abbreviation	XII
Chapter one	
Introduction	1
Problem of study	2
Objectives	2
Significance of the study	3
Chapter two	
Theoretical back ground: Anatomy	4

Physiology	11
Pathology	12
MRI Basic principle and instrumentation	15
Previous study	29
Chapter three	
Materials	30
Methods	31
Chapter four	
Results	34
Chapter five	
Discussion	43
Conclusion	45
Recommendations	46
References	47
Appendices	48

List of figures:

Fig Number	Name of figure	Page
2.1	lobes of the brain	5
2.2	Sagittal section of the brain	6
2.3	Ventricles of the brain	6
2.4	Blood supply of the brain.	8
2.5	Circle of wills.	8
2.6	Parts of corpus callosum.	9
2.7	MRI Image showing parts of corpus callosum	10
2.8	(A) Midsagittal view demonstrating complete agenesis of the corpus callosum; (B) Axial view demonstrating the presence of the non decussating fibre bundles of Probst (medial to the bodies of lateral ventricles - white arrows); (C) Coronal view demonstrating the classic “bat wings” appearance of the lateral ventricles - white arrows.	14
2.9	Midsagittal view demonstrating complete agenesis of the corpus callosum	14

3.1	Sigittal T1 image of male patient (70 Y) showing measurement of various parts of corpus callosum. AB: Fronto-Occipital length, EZ: Corpus Callosum length, AE: Fronto-Corpus Callosum length, ZB: Occipito-Corpus Callosum length	32
3.2	MRI midsagittal brain showing various parts of corpus callosum	33
4.1	A scatter plot diagram shows a linear relationship between the Genu Width and the Age of the subjects, $R^2 = -0.727$.	35
4.2	A scatter plot diagram shows a linear relationship between the Genu Width and the Age of the subjects, $R^2 = -0.395$.	36
4.3	A scatter plot diagram shows a linear relationship between the Splenium Width and the Age of the subjects, $R^2 = -0.000$.	36
4.4	A scatter plot diagram shows a linear relationship between the Fronto-Occipital Length and the Age of the subjects, $R^2 = -0.099$.	37
4.5	A scatter plot diagram shows a linear relationship between the Corpus Callosum Length and the Age of the subjects, $R^2 = -0.082$.	37
4.6	A scatter plot diagram shows a linear relationship	38

	between the Fronto-Corpus Callosum Length and the Age of the subjects, $R^2 = -0.281$.	
4.7	A scatter plot diagram shows a linear relationship between the Occipito-Corpus Callosum Length and the Age of the subjects, $R^2 = -0.396$.	38
4.8	comparison between males and females in Genu Width	39
4.9	comparison between males and females in Trunk Width	40
4.10	comparison between males and females in Splenium Width	40
4.11	comparison between males and females in Fronto-Occipital Length	41
4.12	Comparison between males and females in Corpus Callosum Length.	41
4.13	Comparison between males and females in Fronto-Corpus Callosum Length.	42
4.14	Comparison between males and females in Occipit-Corpus Callosum Length.	42

List of tables:

No	Table title	Page
4.1	Characteristics of subjects enrolled in Magnetic Resonance Imaging studies of the Corpus Callosum:	34
4.2	Table 4.2: Characteristics of subjects enrolled in Magnetic Resonance Imaging studies of the Corpus Callosum per age group:	35
4.3	Table 4.3 comparison between males and females:	39

List of abbreviations:

CC: Corpus Callosum

GE: General Electric

MRI: Magnetic Resonance Imaging

CHAPTER ONE

1.1 Introduction

The corpus callosum is a structure of the mammalian brain in the longitudinal fissure that connects the left and right cerebral hemispheres. It is the largest white matter structure in the brain, consisting of 200-250 million contra lateral axonal projections. It is a wide, flat bundle of axons beneath the cortex. Much of the inter-hemispheric communication in the brain is conducted across the corpus callosum. It is 10 cm long and consists of the rostrum, genu, trunk and splenium. Rostrum is the narrowest part; Genu is the most anteriorly projecting part and lies about 4cm from frontal pole. Trunk (Body) is the main part of corpus callosum. Splenium is the thickened posterior end of corpus callosum and lies about 6 cm from occipital pole. (Standring et al. 2005).

The corpus and its precursors develop between the 8th and 20th gestational weeks, a time during which the cerebral and cerebellar hemispheres are forming. (Arkovich, 1996)

The major function of a corpus callosum is to enhance and maintain communication between brain hemispheres. It plays an integral role in relaying sensory, motor, and cognitive information between two hemispheres; also eye movement, maintaining the balance of arousal and attention. MR imaging enables the in vivo study of cerebral structure and function. Several neuro imaging studies have used the midsagittal area of the corpus callosum to show differences in morphology related to sex, aging and pathologic states. The corpus callosum has been shown to be altered in conditions such as schizophrenia, dyslexia, even when visual assessment of the MR images reveals normal findings. In pathologic

states such as multiple sclerosis and Alzheimer disease, quantitative measures of the corpus callosum have been proposed as useful indicators of disease progression. Several studies indicate that the size and shape of the corpus callosum (CC) in human brain are correlated to sex, age, brain growth and degeneration, handedness, and to various types of brain dysfunction.

1.2 Problem of study:

Corpus callosum is vital part of the human brain because it enhances and maintains communication between brain hemispheres. It is likely to be affected by the physiologic, as well as pathological changes occurred in the regions of brain. Also corpus callosum dimensions and texture might be change in respect to age which generally might insinuate or simulate pathology. Therefore Study of normal measurements of corpus callosum is helpful in providing baseline data for recognizing and diagnosing the presence and progression of diseases as well as to differentiate between degenerative changes and pathological changes.

1.3 Objectives:

1.3.1 General objective:

The main objective of this thesis is to characterize corpus callosum in normal Sudanese population using magnetic resonance imaging (MRI).

1.3.2 Specific objectives:

- To measure the length and width of corpus callosum parts (spllinuom, body and genu).
- To find the association between age, gender in corpus callosum.
- To classify the corpus callosum parts and to find within and between groups difference (in the same age groups and different age groups

- To compare the corpus callosum measurement with the international measurement to find the significant differences.

1.4 Significance of the study

This study will provide a Sudanese index (dimension) for corpus callosum and the associated parts in the normal people and the changes in the measurement that attributed to ageing. As well as the textural identity for the corpus callosum as normal structures which will facilitate the identification of the pathological condition, which might be subtle in the normal visual perception evaluation.

CHAPTER TWO

Theoretical background and Previous study

2.1 Theoretical back ground:

2.1.1 Anatomy:

The brain consist of three main parts the cerebrum, the cerebellum, and the brain stem. The cerebrum consists of two cerebral hemispheres connected by a bundle of nerve fibers, the corpus callosum. The largest and most visible part of the brain, the cerebrum, appears as folded ridges and grooves, called convolutions. The following terms are used to describe the convolutions a gyrus is an elevated ridge, a sulcus is a shallow groove, and a fissure is a deep groove. The deeper fissures divided the cerebrum into five lobes (Figure 2.1) most lobes are named after bordering skull bones: the frontal lobe, the parietal lobe, the temporal lobe, the occipital lobe, and the insula. All but the insula are visible from the outside surface of the brain. The cerebral cortex is a thin outer layer of gray matter.

The cerebral white matter underlies the cerebral cortex. It contains mostly myelinated axons that connect cerebral hemispheres (association fibers), connect gyri within hemispheres (commissural fibers), or connect the cerebrum to the spinal cord (projection fibers). The corpus callosum is a major assemblage of association fibers that forms a nerve tract that connects the two cerebral hemispheres. (M.R.E Dean, 1990)

Basal ganglia are several pockets of gray matter located deep inside the cerebral white matter. The major regions in the basal ganglia—the caudate nuclei, the putamen, and the globus pallidus—are involved in relaying and modifying nerve impulses passing from the cerebral cortex to the spinal cord. The brainstem connects the diencephalon to the spinal

cord. The brainstem resembles the spinal cord in that both consist of white matter fiber tracts surrounding a core of gray matter. The brainstem consists of the following four regions, all of which provide connections between various parts of the brain and between the brain and the spinal cord structures of the brainstem are Midbrain, uppermost part of the brainstem Pons, bulging region in the middle of the brainstem, medulla oblongata , reticular formation, within the white matter of the various regions of the brainstem and certain regions of the spinal cord, diencephalon, and cerebellum. Cerebellum is located dorsal to the pons and medulla and occupies the space between the brain stem and the occipital lobes of the cerebral cortex. It is connected to the brainstem by three peduncles (Vishram Singh. 2004).

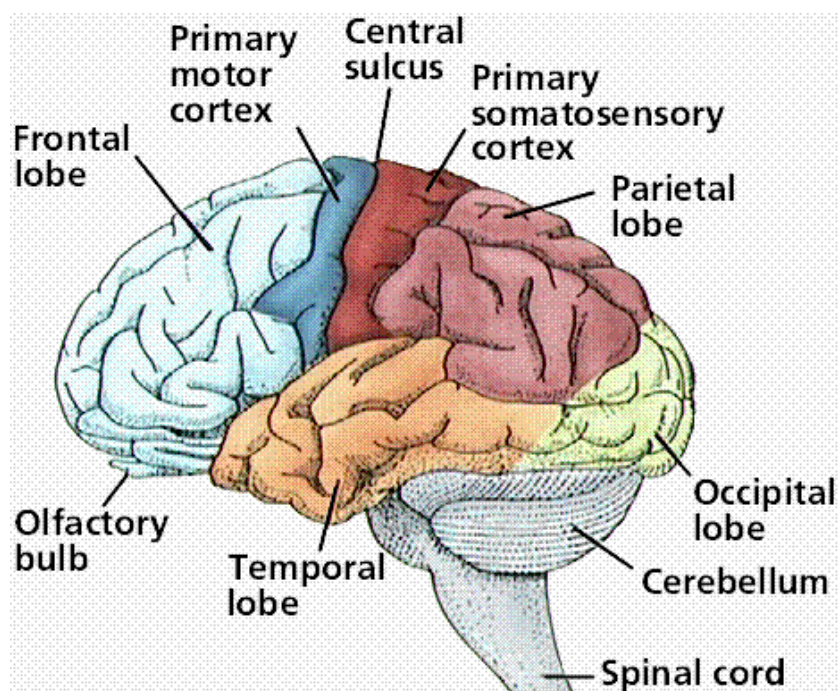


Fig 2.1 lobes of the brain (www.brain-tumoursurgery.co.uk/brain-anatomy/)

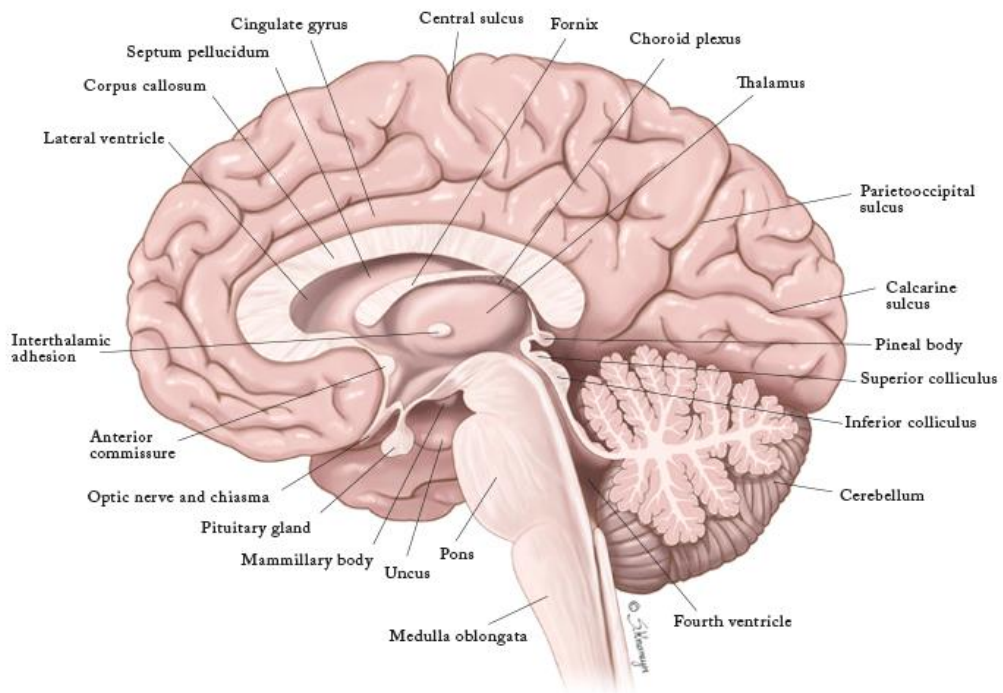


Fig 2.2 Sagittal section of the brain (www.sigrid.knemeyer.com/portfolio/mid-section-of-the-brain/)

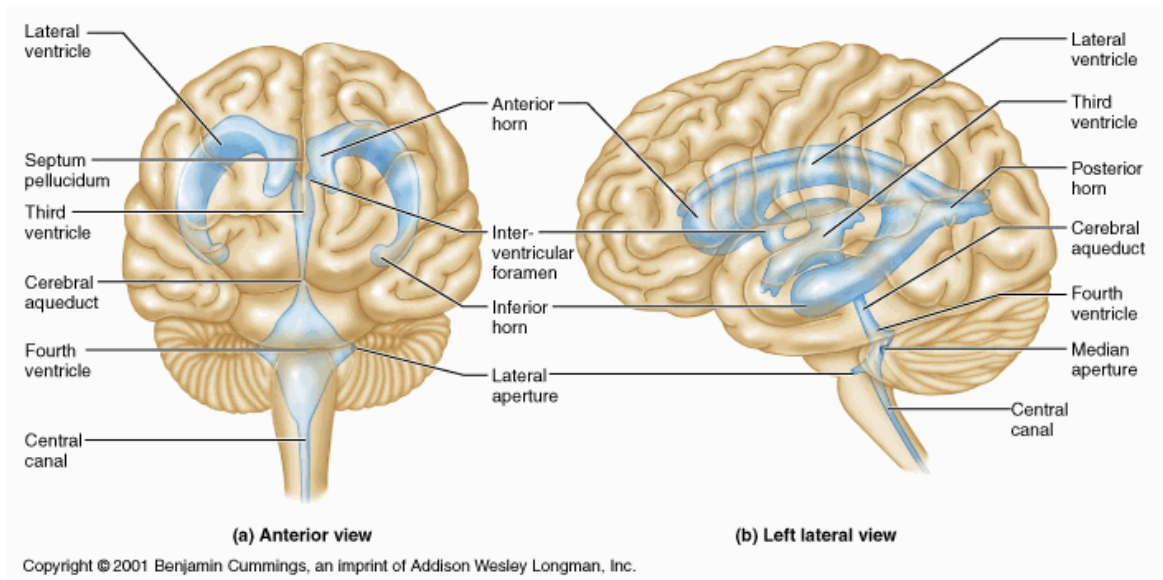


Fig 2.3 Ventricles of the brain

(www.medicallook.com/human_anatomy/organs/ventricles_and_cerebrospinal_fluid.html)

2.1.1.1 Blood supply of brain:-

A. Major Blood Vessels:-

Normal function of the brain's control centers is dependent upon adequate supply of oxygen and nutrients through a dense network of blood vessels. Blood is supplied to the brain, face, and scalp via two major sets of vessels: the right and left common carotid arteries and the right and left vertebral arteries.

The common carotid arteries have two divisions. The external carotid arteries supply the face and scalp with blood. The internal carotid arteries supply blood to the anterior three-fifths of cerebrum, except for parts of the temporal and occipital lobes. The vertebrobasilar arteries supply the posterior two-fifths of the cerebrum, part of the cerebellum, and the brain stem (Vishram Singh.1999).

B. circle of Willis:-

At the base of the brain, the carotid and vertebrobasilar arteries form a circle of communicating arteries known as the Circle of Willis. From this circle, other arteries—the anterior cerebral artery, the middle cerebral artery, the posterior cerebral artery -arise and travel to all parts of the brain. Posterior Inferior Cerebellar Arteries, which branch from the vertebral arteries (Vishram Singh .1999).

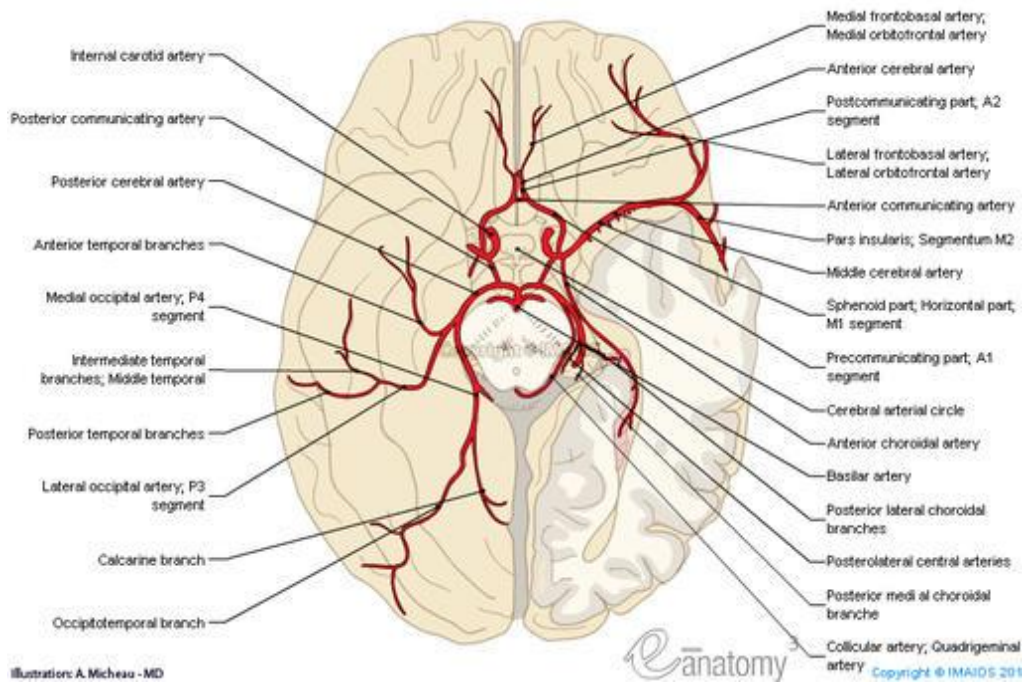


Fig 2.4 Blood supply of the brain.

(www.csuchico.edu/~pmccaffrey//syllabi/cmsd%20320/362unit11.html)

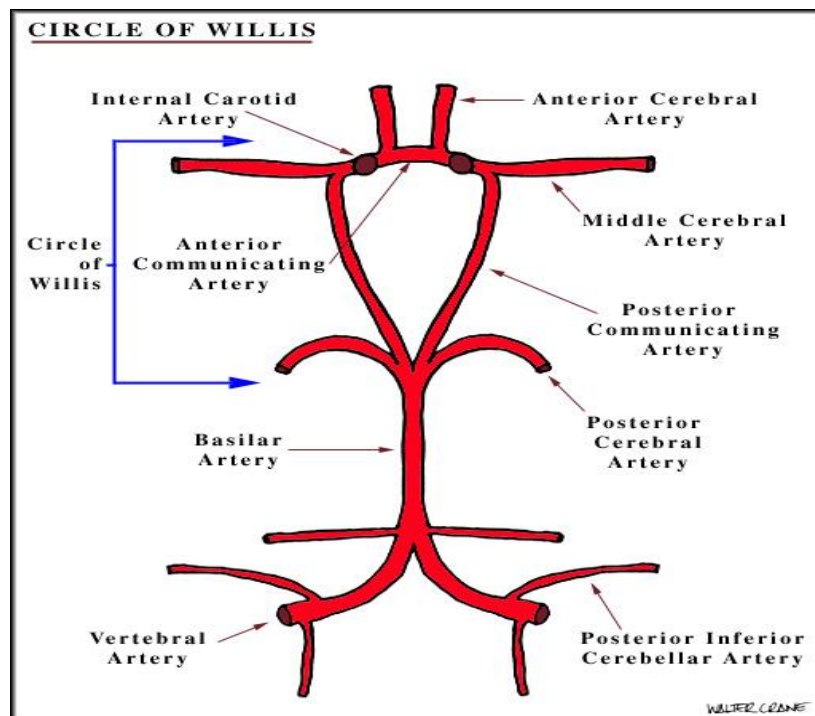


Fig 2.5 Circle of wills.

(www.csuchico.edu/~pmccaffrey//syllabi/cmsd%20320/362unit11.html)

2.1.1.2 Anatomy of corpus callosum:

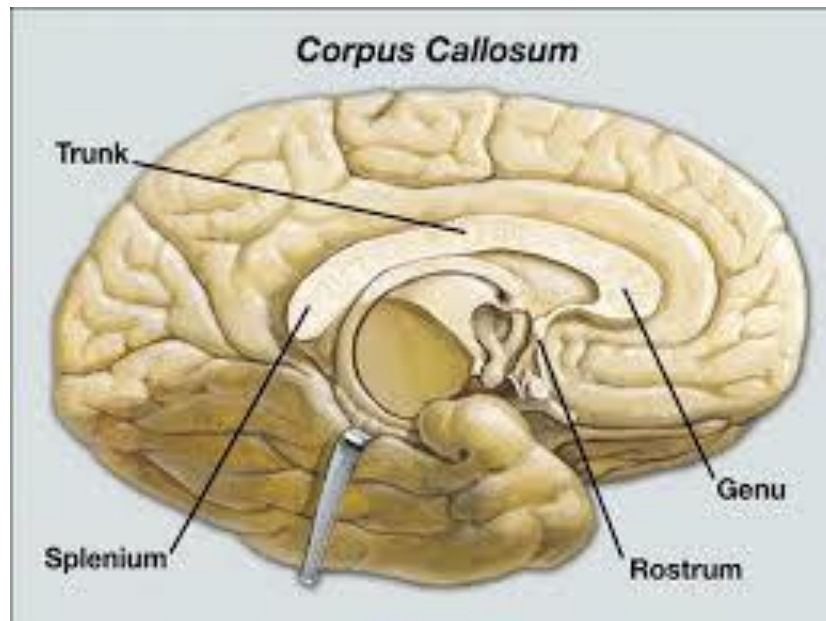


Fig 2.6 Showing parts of corpus callosum. (www.studyblue.com/notes/note/n/25a-gross-brain-i/deck/13404661)

The corpus callosum is unique to placental mammals in the brain structure that connects the right and left hemispheres. It consists of approximately 200 million neural fibers and is responsible for inter hemispheric transfer of information and higher-order cognition. The most parsimonious explanation for callosal evolution is that it arose to facilitate long-distance integration within large brains.

Callosal fibers are first found in human embryos at 10–11 weeks of gestation, and by 12–13 weeks a rudimentary callosal plate can be seen. The corpus callosum first enlarges caudally then develops rostrally. Myelination occurs relatively slowly over the lifespan, with the process completing in puberty. Myelination progresses caudally to rostrally, much as the corpus callosum develops, from the splenium to the genu and

rostrum It begins to develop around the 12th week of gestation and matures through a complex process of neuronal migration, development, and eventual neuronal pruning. By week 20, the corpus callosum can be seen on a sonogram or fetal MRI. Although the corpus callosum may be considered fully developed by around age 4, as with most neural structures, it likely continues to change over the lifespan.

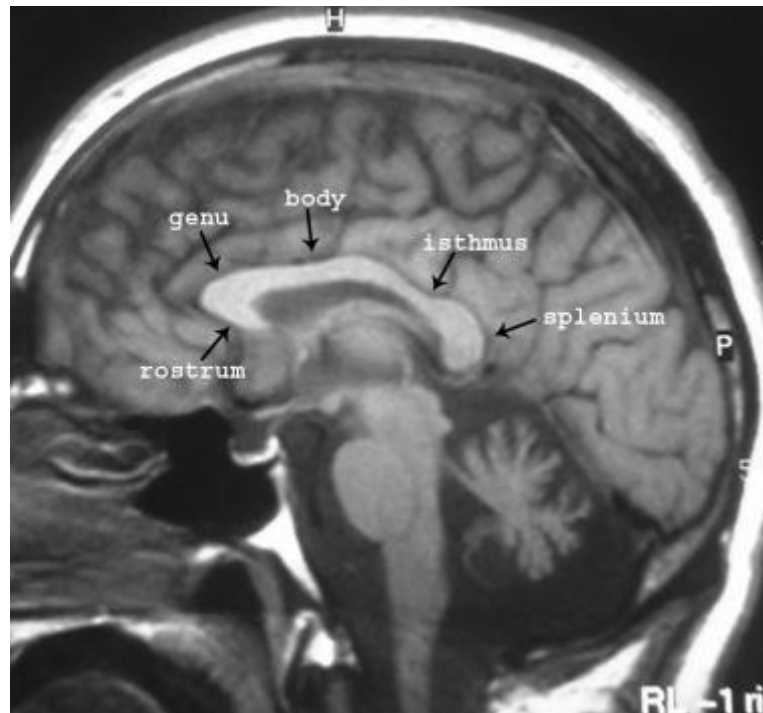


Figure 2.7 MRI Image showing parts of corpus callosum
(www.emedicine.medscape.com/article/407730-overveiu#1)

There are two types of fibers in the corpus callosum. Large diameter fibers mediate sensory-motor coordination whereas small diameter fibers connect association areas. The small diameter fibers are more numerous and individual differences in callosal size have been shown to be a reflection of the small diameter type. It is these small diameter fibers that are thought to be important in maintaining the balance between excitation and inhibition in the cerebral hemispheres.

2.1.2 Physiology:

2.1.2.1 Physiology of brain:

The three main components of the brain—the **cerebrum**, the **cerebellum**, and the **brainstem**—have distinct functions. The cerebrum is the largest and most developmentally advanced part of the human brain. It is responsible for several higher functions, including higher intellectual function, speech, emotion, integration of sensory stimuli of all types, initiation of the final common pathways for movement, and fine control of movement. The left hemisphere controls the majority of functions on the right side of the body; while the right hemisphere controls most of functions on the left side of the body the crossing of nerve fibers takes place in the brain stem. Thus, injury to the left cerebral hemisphere produces sensory and motor deficits on the right side, and vice versa. One hemisphere has a slightly more developed, or dominant, area in which written and spoken language is organized. (Johan .E 2006)

The cerebral cortex or gray matter contains the centers of cognition and personality and the coordination of complicated movements. The gray matter is also organized for different functions. The white matter is a network of fibers that enables regions of the brain to communicate with each other. Such activities as speech, evaluation of stimuli, conscious thinking, and control of skeletal muscles occur here. These activities are grouped into motor areas, sensory areas, and association areas. The cerebellum, the second largest area, is responsible for maintaining balance and finer control of movement and coordination. A stroke involving the cerebellum may result in a lack of coordination, clumsiness, shaking, or other muscular difficulties. The brain stem is the final pathway between cerebral structures and the spinal cord. It is responsible for a variety of automatic functions, such as control of respiration, heart

rate, and blood pressure, wakeful .illness, arousal and attention. (Johan .E 2006)

2.1.2.2 Physiology of corpus callosum:

The major function of a corpus callosum is to enhance and maintain communication between brain hemispheres. It plays an integral role in relaying sensory, motor, and cognitive information between two hemispheres; also eye movement, maintaining the balance of arousal and attention. (Johan .E 2006)

2.1.3 Pathology:

2.1.3.1 Pathology of Brain

Primary CNS neoplasms are the sixth most common tumors in adults, and lesion location, intra axial or extra axial, supratentorial or infratentorial, tumor characterization regular or irregular or calcification, homogeneous or inhomogeneous contrast enhancement and may case mass effect, edema, and brain herniation. Neoplasms divide in primary neoplasms as Glioma, Meningiomas, schwannoma, pituitary adenoma, lymphoma and secondary as metastases, cyst and tumor like lesions. (Howord lee et al 1992)

2.1.3.2 Pathology of corpus callosum:

2.1.3.2.1 Agenesis and Dysgenesis of the Corpus Callosum

Definition:

Agenesis (absence) and dysgenesis (malformation) of the corpus callosum are brain abnormalities involving the large bundle of nerve fibers that connect the two hemispheres of the brain (the corpus callosum). These fibers may be completely absent, partially absent, thin, or malformed in some way.

Although a callosal condition can occur as an isolated diagnosis, it is often associated with other physical, medical, or genetic conditions.

The corpus callosum is important for processing and integrating sensory, motor, and cognitive information. When the corpus callosum is missing or malformed, these functions may be affected. The impact can range from subtle to severe, often depending on additional conditions that may also be present in the individual. Researchers are working to better understand the impact of these disorders and the similarities and differences among and between the different types.

Abbreviation:

ACC (Agenesis of corpus callosum): all or a portion of the corpus callosum is absent.

AgCC(Agenesis of corpus callosum): another abbreviation sometimes used for ACC.

c-ACC (Complete agenesis of the corpus callosum): the entire corpus callosum is absent.

p-ACC (Partial agenesis of corpus callosum): a portion of the corpus callosum is absent.

Dysgenesis of corpus callosum: the corpus callosum is present, but malformed in some way.

Hypogenesis of the corpus callosum: another term used to describe p-ACC.

Hypoplasia of corpus callosum: the corpus callosum is present but abnormally thin.

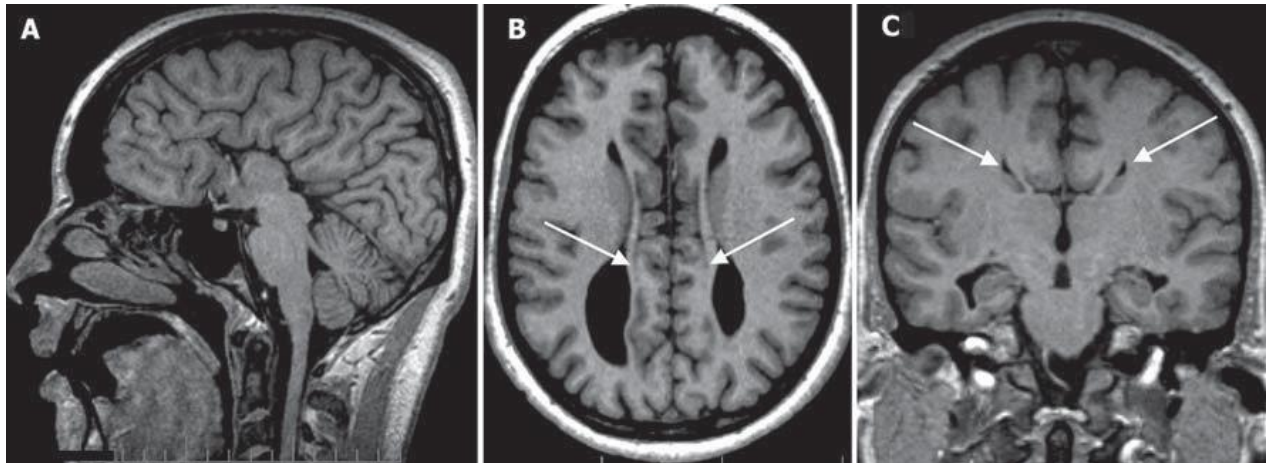


Figure 2.8 (A) Midsagittal view demonstrating complete agenesis of the corpus callosum; (B) Axial view demonstrating the presence of the non decussating fibre bundles of Probst (medial to the bodies of lateral ventricles - white arrows); (C) Coronal view demonstrating the classic “bat wings” appearance of the lateral ventricles - white arrows. (hallak et al., 2007)

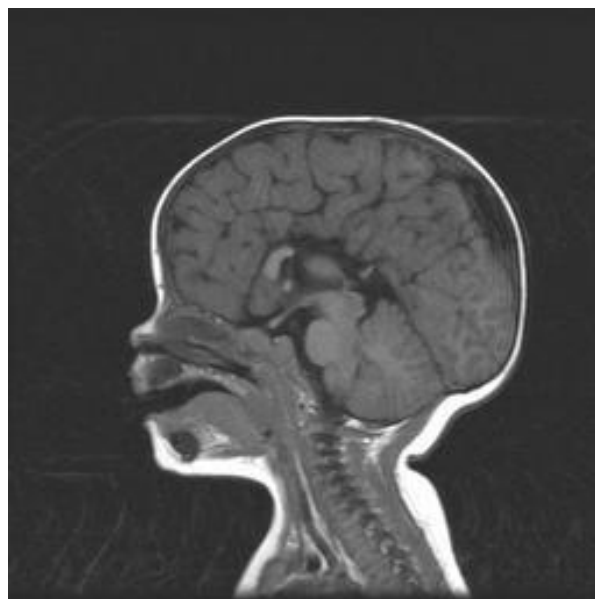


Figure 2.9 midsagittal view demonstrating complete agenesis of the corpus callosum. (www.mypacs.net/cases/agenesis-of-the-corporis-callosum-42781.html)

2.2 MRI Basic principle and instrumentation

2.2.1 Basic Principle of MRI

Magnetic resonance imaging (MRI) is founded on the principle of nuclear magnetic resonance (NMR). The principles of nuclear magnetic resonance are based on the fact that the nuclei of certain elements have a magnetic moment. This means that if a sample of atoms of one of these elements were placed in a magnetic field, its nuclei would tend to line up with the field.

The nuclei don't actually line up exactly in the direction of the magnetic field, however. The laws of quantum mechanics dictate that they align at an angle to the direction of the field.

Each type of nucleus has a quality known as angular momentum associated with it. The idea of an intrinsic angular momentum of the nucleus is fundamental to magnetic resonance imaging. It can be likened to the example of a spinning top. When a top is spun at an angle to the vertical, it will precess about the vertical axis. That is, the top will rotate about its own axis, and the axis of the top's rotation will revolve about the vertical axis.

This precession is due to the angular momentum of the top, which is in turn due to the spinning of the top, in the same way; a nucleus that is aligned at an angle to the direction of the magnetic field will precess about the axis of the field.

The analogy is so exact that the nuclei are commonly referred to as spins that are manipulated to generate images.

In quantum mechanics a number called the spin of the nucleus represents the angular momentum. Depending on the value of the spin number of a

particular, there will be several different orientations in which the nuclei may line up in a magnetic field. Each orientation is representing by a different angle from the direction of the magnetic field about which the nucleus will process.

MRI takes advantage of the fact that the nucleus of a hydrogen atom (a single proton) has a magnetic moment. The spin of the proton is such that the proton has exactly two possible ways to line up with the applied magnetic field. Because of its abundance in the body, hydrogen is a wonderful candidate for use in magnetic resonance imaging.

The frequency at which the nucleus processes is a function of both the strength of the magnetic field and the particular nucleus this frequency, called the larmor frequency, and is equal to the product of the strength of the magnetic field and a constant called the gyro-magnetic ratio. The gyro-magnetic ratio is unique for each nucleus that has a magnetic moment. (Catherine Westbrook, 2008)

The larmor frequency is important, because it's the frequency at which the nucleus will absorb energy that will cause it to change its alignment. In proton imaging this energy is in the radio frequency (RF) range, meaning that the frequency typically varies from(1 to 100)MHz. if an RF pulse at the larmor frequency B_0 applied to a proton, the proton will change its alignment so that rather than being aligned with the main magnetic field, it will be aligned opposite the field. Over a period of time the proton will flip back to align with the field. In doing so, it will emit energy whose frequency is also exactly the larmor frequency. It is this emission of energy that made NMR such a useful means to locate on image protons(Catherine Westbrook, 2008).

The term resonance refers to that property of the procession nucleus in which it absorbs energy only at the larmor frequency. If the frequency is off even by a small amount, the nucleus will not absorb any energy, nor will it change state. (Catherine Westbrook, 2008)

2.2.2 MRI Instrumentation:

The MRI system consists of, the magnet, the gradient coils, the radiofrequency subsystem and the computer. (Catherine, 2008)

2.2.2.1 The Magnet:

The heart of all MR system is the magnet. There are three types of the magnets in common use for MRI; all have in common that they can generate large uniform magnetic fields. They differ in the cost to produce the magnet, the strength that can be produced, energy requirement to support the magnet, and the direction of the main magnetic fields. (Catherine, 2008)

A. Super Conducting Magnets: -

By far the most commonly used magnet is the superconducting magnet. This type of magnet is notable in that the magnetic field can be maintained for a very long period of time without requiring a constant source of energy. This allows the use of this type of magnet in systems that require extremely strong magnetic field (above 0.5 T). (Catherine, 2008)

A superconducting magnet consists of many winding of wire that carries on electric current. The magnet field generates by this cylinder of wires runs in the direction along the long axis of the cylinder. When used to produces MR. Images the superconducting magnet produces relatively high magnetic field strength with low power requirement. (Catherine, 2008)

B. Resistive Magnets: -

Resistive magnets are similar to superconducting magnets, in that they are typically coils of wire through which a magnetic field is induced. However, the wires aren't cooled to a superconductive state. Therefore, the wires are resistive, and if a current were applied and the power supply disconnected the current would eventually die out.

The major difference, therefore, is one of tradeoffs in operating cost. A resistive magnet doesn't require liquefied gases (cryogenes), but it does require a power supply to keep the magnet at a stable field. As a result of the increase in cost, these magnets aren't seen in commercial systems at field strengths over 0.4 T. (Catherine, 2008)

C. Permanent Magnets

The permanent magnet is gaining in popularity for systems that operate at magnetic fields up to about 0.4T. A large part of this popularity is due to the fact that a permanent magnet has few requirements to maintain it. While a superconducting magnet requires cryogenes, and a resistive magnet requires a power supply to maintain its current a permanent magnet requires neither.

The disadvantages of using a permanent magnet are its weight and the cost of the magnet and supporting structure. In addition, permanent magnets are susceptible to hysteresis (a time varying change in the field). They are commonly used now for low cost systems; the cost (and weight) of the magnets has precluded their use at higher field strengths. (Catherine, 2008)

2.2.3 Types of Coils according to the usage:

2.2.3.1 Shim Coils:

Due to design limitation it's almost impossible to create an electromagnet, which produces a perfectly homogeneous magnetic field. To correct for these inhomogeneities, other loop of current carrying wire are placed around the bore. This process is called shimming and the extra loop of wire is called a shim coil. Shim coils produce magnetic field evenness or homogeneity. For imaging purposes, homogeneity of the order of 10 ppm is required. Spectroscopic procedures require a more homogeneous environment of 1 ppm.

The shim system requires a power supply which is separate from the other power supplies within the system. This is important because a fault in the shim power supply compromises image quality. (Catherine, 2008)

2.2.3.2 Gradient Coils:

The magnetic field strength is proportional to the amount of current passed through the loop of wire, the number of loops in the wire, the size of the loops, and how closely the loops are spaced. If the loops are spaced closely at one end of the solenoid and gradually become farther apart at the other end, the resultant magnetic field becomes stronger at one end than the other. This is called a magnetic field gradient. Gradient coils provide a linear gradation or slope of the magnet field strength from one end of the solenoid to the other. The gradient is applied by passing current through the gradient coils in a certain direction. The amplitude of the gradient slope is determined by the magnitude of the current passing through the coil. (Catherine, 2008)

By varying the magnetic field strength, gradient provide position dependent variation of signal frequency and are therefore used for slice

selection, frequency encoding, phase encoding, rewinding and spoiling. Gradient coils are powered by gradient amplifiers. Faults in the gradient coils or gradient amplifiers can result in geometric distortion in the MR image. (Catherine, 2008)

2.2.3.3 Radio Frequency Coils:

The energy required to produce resonance of nuclear spins is expressed as a frequency and can be calculated by the Larmor equation. At field strengths used in MRI, energy within the radio frequency (RF) band of the electromagnetic spectrum is necessary to perturb or excite the spins. As shown by the Larmor equation, the magnetic field strength is proportional to the RF, the energy of which is significantly lower than that of X-rays. In order to produce an image, RF must first be transmitted at the resonant frequency of hydrogen so that resonance can occur. The transverse component of magnetization created by resonance must be detected by a receiver coil. (Catherine, 2008)

The configuration of the RF transmitter and receiver probes or coil directly affects the quality of the MR signal. There are several types of coils currently used in MR imaging. These are:

A. Volume Coils

A volume coil both transmits RF and receives the MR signal and is often called a transceiver. It encompasses the entire anatomy and can be used for either head or total body imaging. Because of their large size they generally produce images with lower SNR than other types of coils. (Catherine, 2008)

B. Surface Coils :

Coils of this type are used to improve the SNR when imaging structures near the surface of the patient (Such as lumbar spine). As the SNR is enhanced when using local coils (surface coils) greater spatial resolution of small structures can often be achieved when using local coils, the body coil is used to transmit RF and the local coil is used to receive the MR signal. (Catherine, 2008)

C. Phase Array Coils:

Phased array coils are now widely used. These consist of multiple coils and receivers whose individual signals are combined to create one image with improved SNR and increased coverage. Therefore the advantages of small surface coil (increased SNR and resolution); can be combined with a large FOV for increased anatomy coverage. Usually up to four coils and receiver are grouped together to increase either longitudinal coverage (for spin imaging), or to improve uniformity across a whole volume (pelvic imaging). (Catherine, 2008)

D. Circumferential Coils:

At the point where depth equals radius of the structure being imaged, the coil may be placed around the object in a circumferential fashion to form a solenoid. Circumferential coils provide good signal responses across the image because all points are within one radius from the edge of the coil. Two general configurations are possible with circumferential coils: solenoidal and saddle. It can be used to image the neck, knee, ankle and pediatric. (Catherine, 2008)

2.2.3.4 The computer system

MRI computer systems vary with manufacture. Most however consist of:

Aminic computer with expansion capabilities, An array processor for Fourier transformation. An image processor that takes data from the array processor to form an image. Hard disc drives for storage of raw data and pulse sequence parameters. A power distribution mechanism to distribute and filter the alternating current. (Catherine, 2008)

Conventional spin echo:

The spin echo sequence is utilizes a 90° excitation pulse to flip the net magnetization vector (NMV) into the Transverse plane. The NMV precesses in the transverse plane, inducing a voltage in the receiver coil. The precession paths of the magnetic moment of the nuclei within the NMV are translated into the transverse plane. When the 90° RF pulse is remove a free induction decay signal (FID) is produced. T2 dephasing occurs immediately and the signal decays. A 180° RF pulse is then used to compensate for this dephasing.

Spin echo pulse sequences are the gold standard for most imaging. They may be used for almost every examination. T1 weighted images are useful for demonstrating anatomy because they have a high signal to noise ratio (SNR). In conjunction with contrast enhancement however, they can show pathology. T2 weighted also demonstrate pathology. Tissues that are diseased are generally more edematous and/or vascular. They have increased water content and consequently, have high on T2 weighted image and can therefore be easily identified. The conventional spin echo has the advantages of good image quality, very versatile and true T2

weighted sensitive to pathology. They have the disadvantages of requiring longer scan time. (Catherine, 2008)

2.2.3.5 Fast Spin Echo (Turbo Spin Echo):

As the name suggests, fast spin echo (FSE) is a spin echo pulse sequence, but with scan times that are drastically shorter than conventional spin echo.

As the scan time is a function of the TR, NEX and number of phase encoding, in order to reduce the scan time, one or more of these factors should be reduced. Decreasing the TR and the NEX affects image weighting and SNR which is undesirable. Reducing the number of phase encodings reduces the spatial resolution, which is also a disadvantage. In fast spin echo, performing more than one phase encoding step and subsequently filling more than one line of K space per IR reduce the scan time. This is achieved by using an echo train that consists of several 180°-rephrasing pulses, at each rephrasing an echo is produced and a different phase encoding step is performed. (Catherine, 2008)

In conventional spin echo, raw image from each echo stored in K space, and the numbers of 180° rephrasing pulses applied corresponds to the number of echoes produced per TR. Each echo is used to produce a separate image. In fast spin echo, data from each echo is placed into one image. The number of 180° rephrasing pulses performed per TR corresponds to the number is called the turbo factor or the echo train length. As the turbo factor increase, the scan time decrease, as more phases encoding steps are performed per TR. (Catherine, 2008)

The advantages of the fast spin echo is that, the scan times greatly reduced, high-resolution matrices and multiple NEX can be used, and image quality improved, and increased T2 information.

The disadvantages are some flow and motion affects increased, incompatible with some imaging options, fat bright on T2 weighted images, image blurring can result as data is collected at different TE times, reduce magnetic susceptibility effect as multiple 180° pulses produce excellent rephasing so it should not be used when haemorrhage is suspected

In recent years, fast spin echo (FSE) sequences have begun to replace conventional spin echo sequences. (Catherine, 2008)

2.2.3.6 The Gradient Echo Pulse Sequence:

A gradient echo pulse sequences utilizes an RF excitation pulses that is variable, and therefore flips the NMV through any angle (not just 90°). A transverse component of magnetization is created, the magnitude of which is less than in spin echo, where all the longitudinal magnetization is converted to the transverse plane. When a flip angle other than 90° is used only part of the longitudinal magnetization is converted to transverse magnetization, which precesses in the transverse plane and induces a signal in the receiver coil.

Gradient echo pulse sequences can be acquired T2*, T1 and proton density weighted, however, there is always some degree of T2* weighted present on any image due to the absence of 180° rephrasing pulse. Gradient echo sequence allow for reduction in the scan time as the TR is greatly reduced. They can be used for signal slice breath-hold acquisition in the abdomen, and for dynamic contrast enhancement. They are very sensitive to flow as gradient rephrasing is not slice selective, so flowing nuclei always give a signal, as long as they have been previously excited. Because of this, gradient echo sequences may be used to produce angiography, type images.

They provide interesting capabilities in term of contrast and speed. These techniques can be broadly divided into " steady state " sequences, such as gradient recalled steady state (GRASS) and fast imaging with steady state free precession (FISP), and " spoiled " sequences, such as fast low-angle signal-shot (FLASH) and (spoiled GRASS). (Catherine, 2008)

2.2.3.7 Three-Dimensional Fourier Transform (3DFT):

The great attraction of this technique is that a high resolution volume data set can be processed retrospectively to generate any arbitrarily oriented plane of section. For instance, a radial image can be produced using suitable software. Three-dimensional acquisition is only practical with fast scan sequences.

The advantages of 3DFT imaging are the ability to acquire thin section without gabs and the potential for 3D rendering and reformatting. The disadvantages of 3DFT imaging is that the costs include a significantly lager requirement for resources such as computing power, memory, display, and storage. Other less well-established concerns are that the examinations may take longer to interpret, given that more sections must be viewed, and that there may be a penalty in signal-to-noise and contrast, which accompanies the requirement. (Catherine, 2008)

2.2.3.8 Inversion Recovery:

Inversion recovery is a pulse sequences that begins with a 180° inverting pulse. This inverts the net magnetization vector (NMV) through 180° into full saturation. When the inverting pulse is removed the NMV begins to relax back to B_0 .

A 90° excitation pulse is then applied at a time from the 180° inverting pulse know as time from inversion (I 1). The contrast of the resultant

image depends primarily on the length of the TI. If the 90° excitation pulse is applied after the NMV has relax back through the transverse plane the contrast in the image depend on, the amount of longitudinal recovery of each vector (as in spin echo). The resultant image is heavily Ti weighted, as the 180° inverting pulse achieves full saturation and ensure a large contrast difference between fat and water.

If the 90° excitation pulse is not applied until the NMV has reached full recovery, a proton density image result, as both fat and water have full relaxed.

After the 90' excitation pulse, a 180°rephasing pulse is applied at a time TB after excitation pulse. This produces a spin echo. The TR is the time between each 1800 inverting pulse.

Inversion recovery is used to produce heavily Ti weighted images to demonstrate anatomy. The 180° inverting pulse produce a large contrast difference between fat and water because full saturation of the fat and water vectors is achieved at the beginning of each repetition. Inversion recovery pulse sequences therefore produce more heavy T1 weighting than conventional spin echo and should be used when this is required. As the use of contrast primary shortens T1 times of certain tissue, IR pulse sequences increase the signal from structures that have enhanced as a result of a contrast injection.

Inversion recovery has the advantages that it gives very good SNR, as the TR is long and excellent T1 contrast. The disadvantage that is it spends along scan times unless used in conjunction with fast spin echo. (Catherine, 2008)

2.2.3.9 STIR (short T1 inversion recovery):

Is an inversion recovery pulse sequence that uses a T1 that corresponds to the time it takes fat to recover from full inversion to the transverse plane so that there is no longitudinal magnetization corresponding to fat, When the 90° excitation pulse is applied, the fat vector is flipped through 90° to 180° and into full saturation, so that the signal from fat is nulled. STIR is used to achieve suppression of the fat signal in a T1 weighted image.

One of the advantages of STIR is that it is relatively reliable and system independent. As in spin echo, the contrast mechanism can be fairly easily reproduced from system to system and field strength to field strength, with appropriate correction of timing parameters. (Catherine, 2008)

The primary disadvantages lies with scan time. STIR scan time, as for inversion recovery sequences, can be computed as the product {TR x NEXx Matrix}. Since relatively long TR values are generally used, this resultant in scans times comparable to even longer than standard T2 weighted spin echo sequences. (Catherine, 2008)

In addition, we must be careful in the use contrast agent in conjunction with STIR sequences. Gadolinium will shorten the T1 relaxation rate for vascularity, its T1 value will not be affected, and however, fatty lesions may experience some T1 shortening and therefore have reduced effectiveness in fat suppression. The combination of STIR with gadolinium enhancement has proven useful in the evaluation of breast lesion where sufficiently suppression of the fat signal combined with enhancement of the lesion has been shown to increase delectability. (Catherine, 2008)

2.2.3.10 Spectral pre-saturation Inversion Recovery (SPIR):

This method is a combination of the spectral saturation and (STIR) routines it is available on Philips scanners where it is designated Spectral Inversion Recovery (SPIR and GE scanners with the designation Spectral Inversion at Lipids (SPECIAL). The idea is to apply a spectrally selective pulse to flip fat spins then, after the time interval that lets the Mz of fat reach zero, the excitation pulse is applied and the signal of the water spins give most of the signal.

Time is the major disadvantage of this fat suppression method. The routine is best applied at least once per TR, and for multi-slice sequences once per slice per TR. The best fat suppression is achieved with a 180 degree spectral inversion pulse and a time delay equal that used in normal STIR imaging (approximately 150 msec at 1.5 T) plus the finite time required for the inversion pulse) This is clearly impractical for anything but extremely long TR techniques.

In practice the 'inversion' pulse used ranges between slightly more than 90 degrees but significantly less than 180 degrees the required delay time can be acceptably short. In most scanners using this method the radiographer has control of the inversion flip angle and the system determines the optimum delay time The routine is applied in a "segmented" fashion allowing some small variation in the degree of fat suppression across slices.

SPIR will be as sensitive to local field inhomogeneity as spectral saturation routines. It is suitable for use after Gd contrast because only the fat spins are affected by the routine. (Catherine, 2008)

2.3 Previous Studies:

Laissy J. P. et al (1993) in their study they found the Mean CC midsagittal surface area was 6.36 cm^2 , and mean length was 70.6 mm. Mean diameters for the genu, the body, and the splenium were respectively 9.6, 6, and 10.8 mm. The MISS was 143.19 cm^2 and the CC/MISS ratio 4.46%. Average CC/subcutaneous fat ratio was 0.7 (SD, 0.06). CC/CSF ratio was 3.45 (SD, 0.5).

Ronald A. Rauch and J. Randy Jenkins (1995) in their study they found the mean callosal area for all subjects was 5.7 cm^2 . The average SD for each series of measurements from one image made by one observer was 0.20 cm^2 . With these data, the calculated 95% confidence interval for any one measurement was 62.5%. The average SD for mean callosal areas measured from different images of the same subject was 0.26 cm^2 . With these data, the calculated 95% confidence interval for any one image's measurement was 63.7%.

Mohammadi MR et al. (2011) in their study they found the mean value for the longitudinal dimension of the brain (AB) was $161.2 \pm 0.081 \text{ mm}$ (95% CI; 15.96-16.28), while the mean value for the longitudinal dimension of the CC (EZ) was $70.6 \pm 0.52 \text{ mm}$ (95% CI; 6.96-7.17), a ratio greater than 2:1. The mean value for the longitudinal dimension of the genu (EZ/3) and the splenium (EZ/5) was $23.5 \pm 0.17 \text{ mm}$ (95% CI; 2.316-2.385) and $14.1 \pm 0.10 \text{ mm}$ (95% CI; 1.388- 1.429), respectively. The distance between the genu and the frontal pole (AE) had a mean value of $36.8 \pm 0.34 \text{ mm}$ (95% CI; 3.616-3.751), while the distance from the splenium to the occipital pole (BZ) was $55.80 \pm 0.52 \text{ mm}$ (95% CI; 5.476-5.485), an approximate ratio of 1:1.5. The mean value for the distance between the upper and lower surfaces of the brain (CD-vertical diameter) was $106.3 \pm 5.1 \text{ mm}$.

CHAPTER THREE

Materials and methods

3.1 Materials:

This study was carried out using MRI scanner of 1.5 Tesla (Toshiba and GE) in the period from August 2015– 2016.

3.1.1 Design:

This study is a descriptive cross-sectional study conducted at Modern Medical Center, Al-zaytona Hospital, and Royal Care International Hospital.

3.1.2 Population:

This study included male and female with normal corpus callosum their age ranged between 10-74 years. Patients were excluded only when the pathologic process affected, or theoretically could affect, the corpus callosum (e.g., hydrocephalus or tumor) and when the entire corpus callosum was not on a single slice as a consequence of an oblique imaging plane. Magnetic resonance images were eliminated if there was any visible evidence of deviation from the midsagittal plane.

3.1.3 Sample size and type:

A convenient sample type will be adapted, where a total of 50 patients (25 male and 25 female) present for Brain MRI scan will be included in the study in respect to the inclusion criteria.

3.2 Methods:

3.2.1 Techniques:

Patient undergo to MRI department for MRI brain, use the head coil with a sheet on the table, remove dentures, hair clips, hair combs, earrings, nose rings, necklaces, position the patient so their head and neck are relaxed, but without rotation in either plane, centre the field of view on the nasion in the midline, making minor adjustments for baseline tilt.

3.2.2 Measurement:

Data collection sheet will be used to collect data about demographic characteristics (gender and age).

In this study various parameters of corpus callosum were measured in people at the mid-sagittal plane of magnetic resonance imaging as follows:

- Thickness and length of various parts of corpus callosum at its maximum level (genu, body and splenium).
- Maximum length and maximum width of corpus callosum.
- Distance of corpus callosum from frontal pole and occipital pole of cerebral hemisphere.

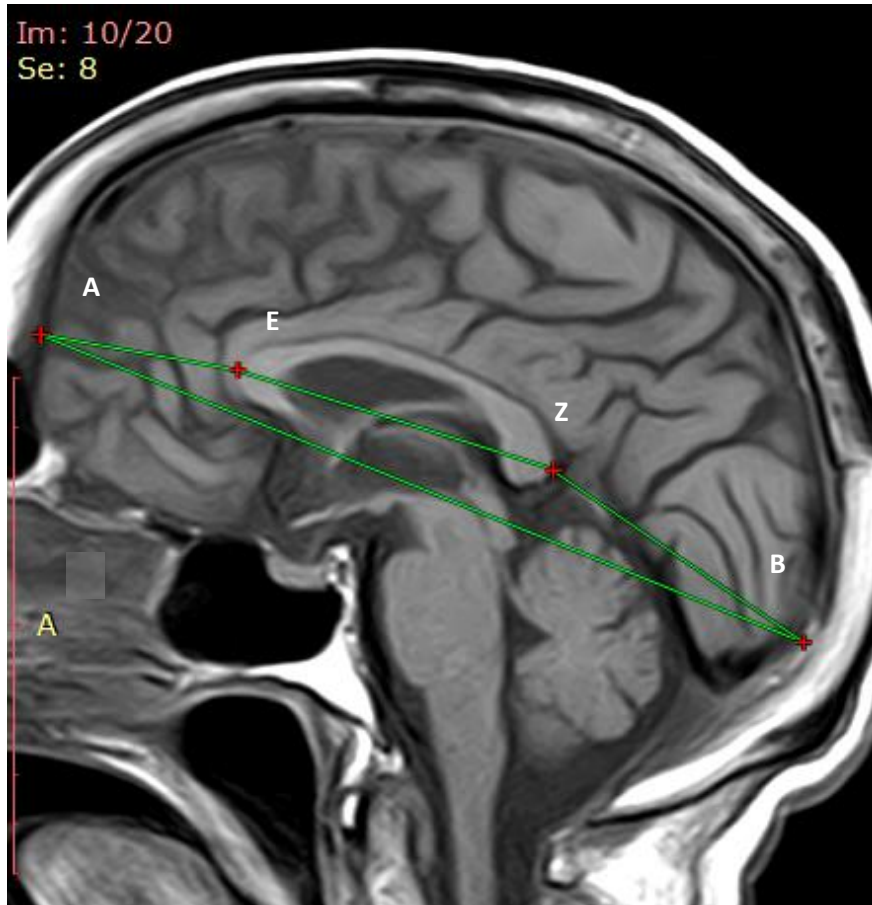


Figure 3.1 Sagittal T1 image (TR: 676, TE: 10, slice thickness: 5.3 mm) of male patient (70 Y) showing measurement of various parts of corpus callosum. AB: Fronto-Occipital length, EZ: Corpus Callosum length, AE: Fronto-Corpus Callosum length, ZB: Occipito-Corpus Callosum length

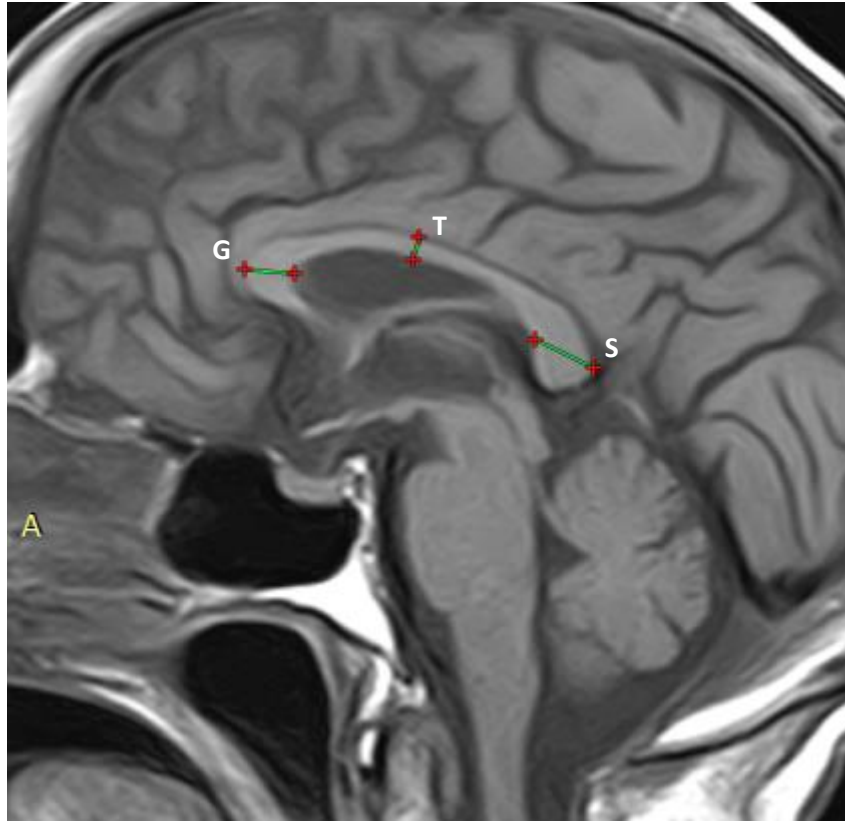


Figure 3.2 Sagittal T1 image (TR: 676, TE: 10, slice thickness: 5.3 mm) of male patient (70 Y) showing measurement of various parts of corpus callosum. G: the Genu, T: the Trunk, S: the Splenium

3.2.3 Method of data analysis:

The data will be analyzed using Excel (scatter plots depict the relationship of the corpus callosum measurement with the age and gender) and SPSS histogram plots with the mean, standard deviation, and normal curve superimposed as well as significant differences between the different age groups and the international measurement.

CHAPTER FOUR

Results

Table 4.1: Characteristics of subjects enrolled in Magnetic Resonance Imaging studies of the Corpus Callosum:

	Total	Minimum	Maximum	Males	Females
Age (years)	37.04 +/- 18.72	10	70	35.64 +/- 18.49	38.44 +/- 19.21
Genu Width (mm)	11.63 +/- 1.77	10.5	12.1	11.47 +/- 1.68	11.80 +/- 1.88
Trunk Width (mm)	6.04 +/- 1.18	5.77	6.2	6.28 +/- 1.17	5.79 +/- 1.16
Splenium Width (mm)	11.37 +/- 1.85	11.05	12.3	11.36 +/- 2.17	11.38 +/- 1.52
Fronto-Occipital Length (mm)	159.59 +/-1.85	157.1	160.8	162.80 +/- 7.76	156.38 +/- 6.22
Corpus Callosum Length (mm)	73.76 +/- 6.84	72.5	76.1	75.08 +/- 6.01	72.44 +/- 7.46
Fronto-Corpus Callosum Length (mm)	35.67 +/- 3.18	33.6	36.9	36.88 +/- 3.04	34.46 +/- 2.88
Occipito-Corpus Callosum Length (mm)	51.10 +/- 5.61	47.9	53.4	52.41 +/- 5.71	49.80 +/- 5.29

Table 4.2: Characteristics of subjects enrolled in Magnetic Resonance Imaging studies of the Corpus Callosum according to age group:

Age group	Mean and SD of Age	Genu Width (mm)	Trunk Width (mm)	Splenium Width (mm)	Fronto-Occipital Length (mm)	Corpus Callosum Length (mm)	Fronto-Corpus Callosum Length (mm)	Occipito-Corpus Callosum Length (mm)
10-30	21.0±6.3	12.02±1.7	6.07±1.1	11.05±2.0	160.8±8.5	72.55±4.9	36.98±3.0	53.47±5.8
31 -50	40.0±7.09	12.14±1.4	6.27±1.1	12.33±1.2	157.18±5.9	76.16±4.0	33.68±2.8	47.95±4.9
51-70	61.92±7.7	10.52±1.7	5.77±1.2	11.07±1.68	159.50±7.3	73.75±10.5	35.11±2.9	49.75±3.1

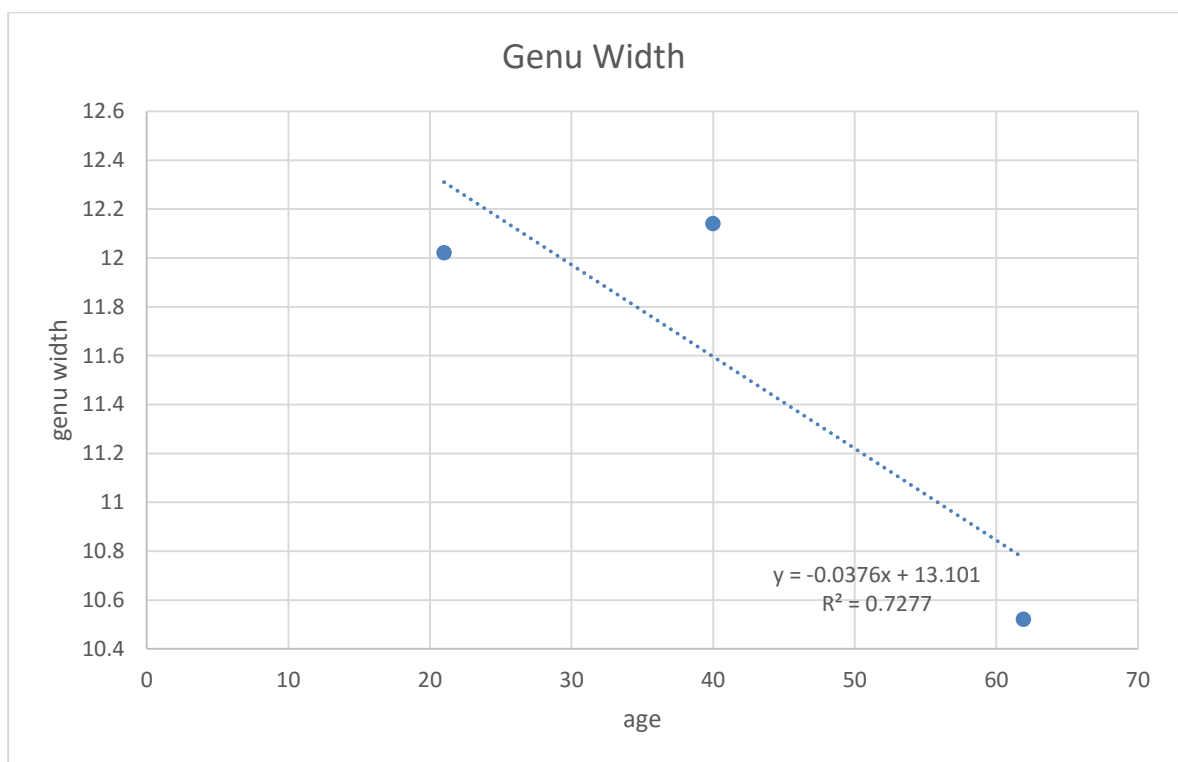


Figure 4.1 A scatter plot diagram shows a linear relationship between the **Genu Width** and the **Age** of the subjects, $R^2 = 0.727$.

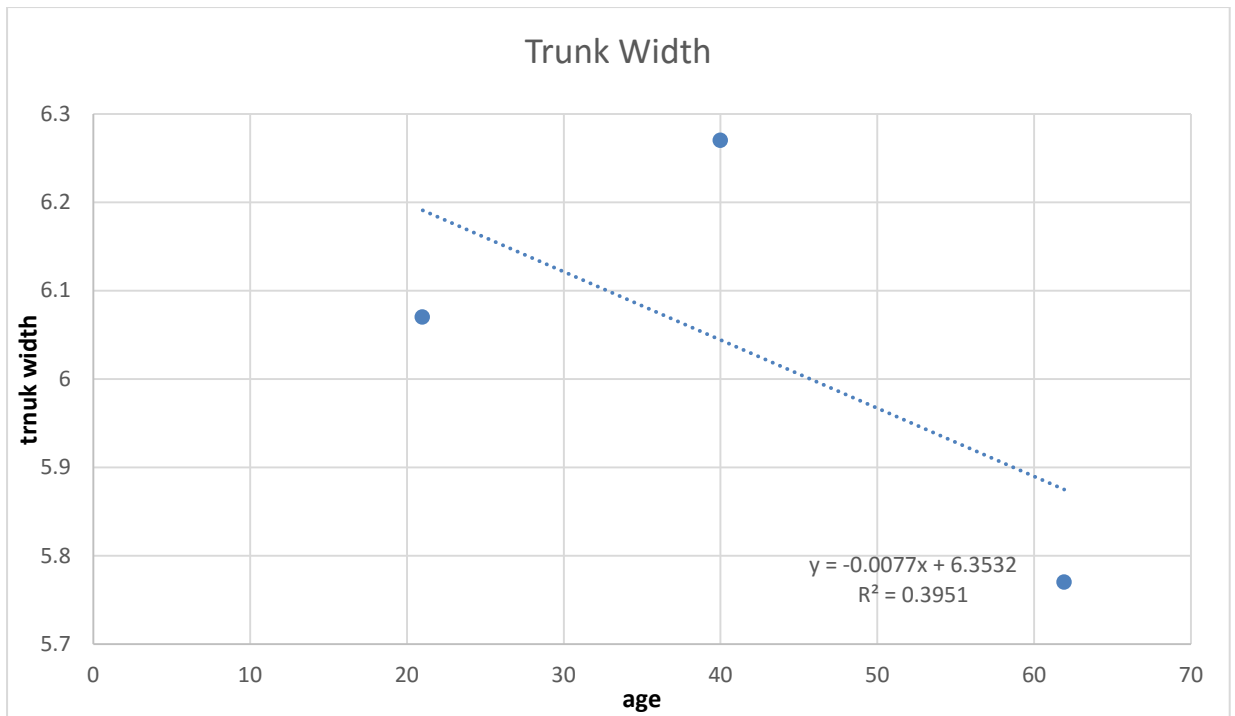


Figure 4.2 A scatter plot diagram shows a linear relationship between the **Genu Width** and the **Age** of the subjects, $R^2 = -0.395$.

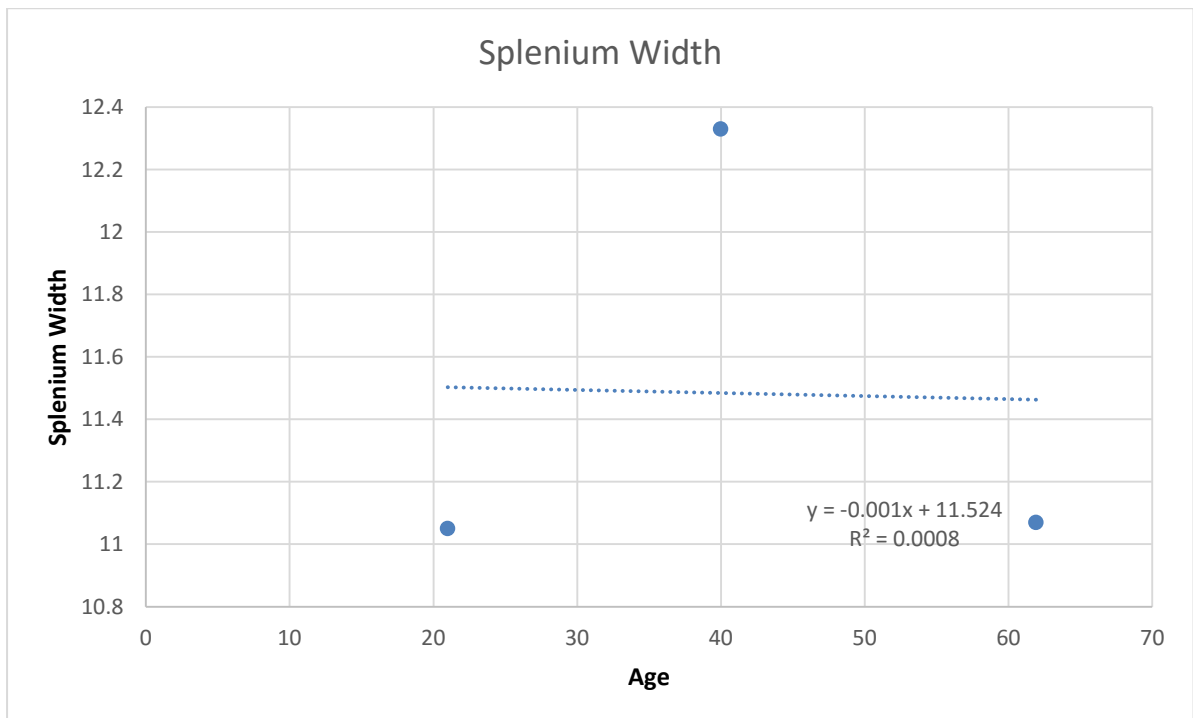


Figure 4.3 A scatter plot diagram shows a linear relationship between the **Splenium Width** and the **Age** of the subjects, $R^2 = -0.000$.

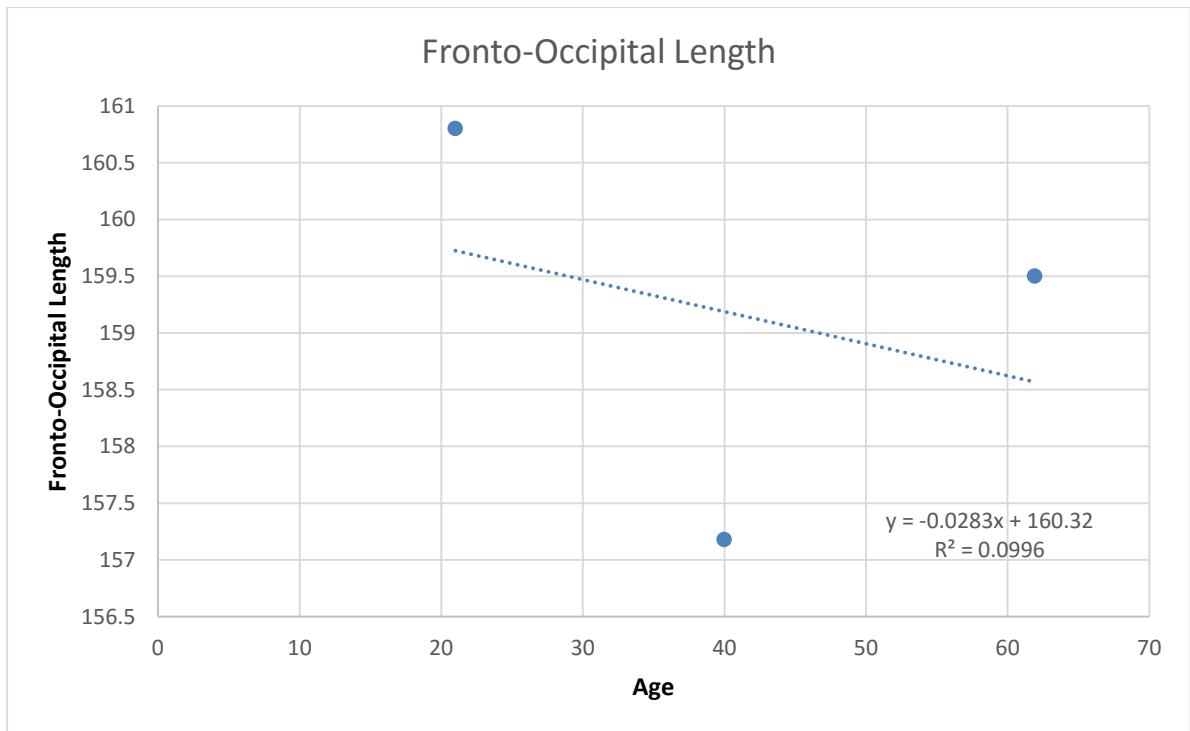


Figure 4.4 A scatter plot diagram shows a linear relationship between the **Fronto-Occipital Length** and the **Age** of the subjects, $R^2 = -0.099$.

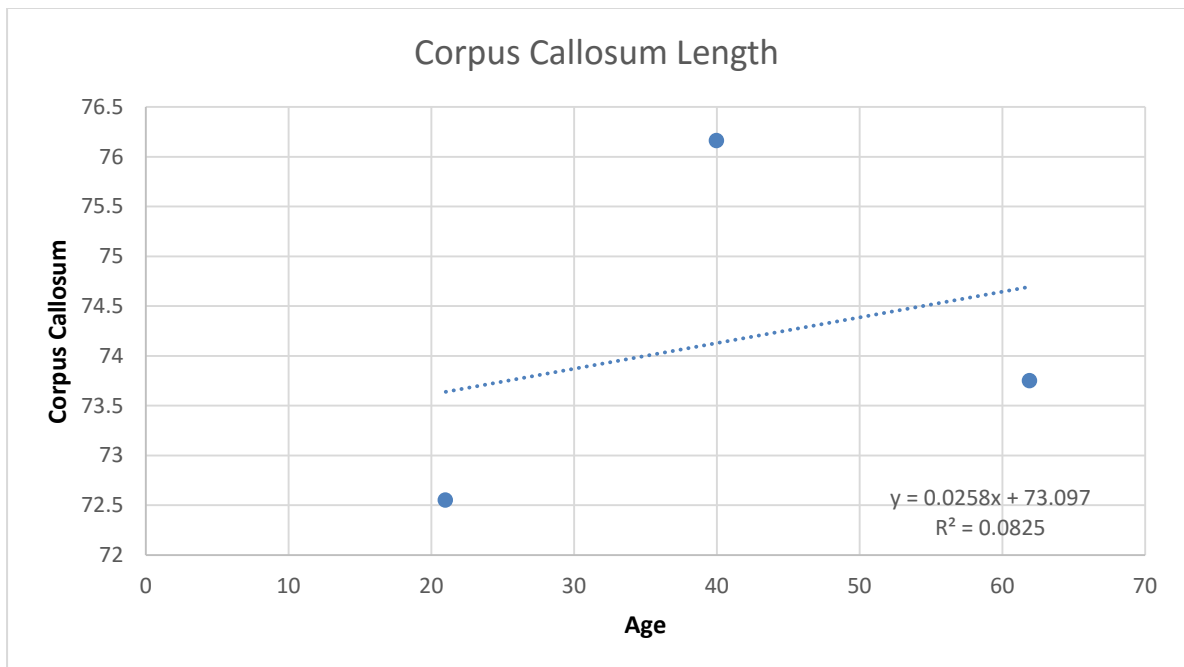


Figure 4.5 A scatter plot diagram shows a linear relationship between the **Corpus Callosum Length** and the **Age** of the subjects, $R^2 = 0.082$.

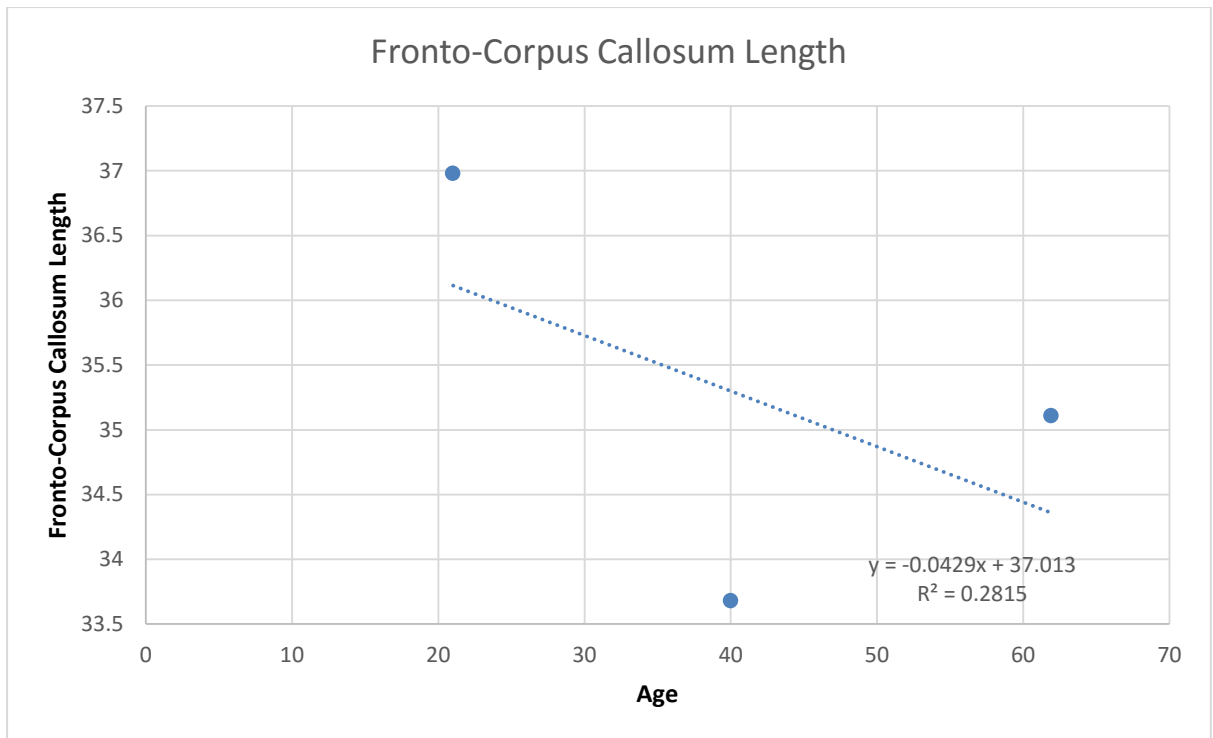


Figure 4.6 A scatter plot diagram shows a linear relationship between the **Fronto-Corpus Callosum Length** and the **Age** of the subjects, $R^2 = 0.2815$.

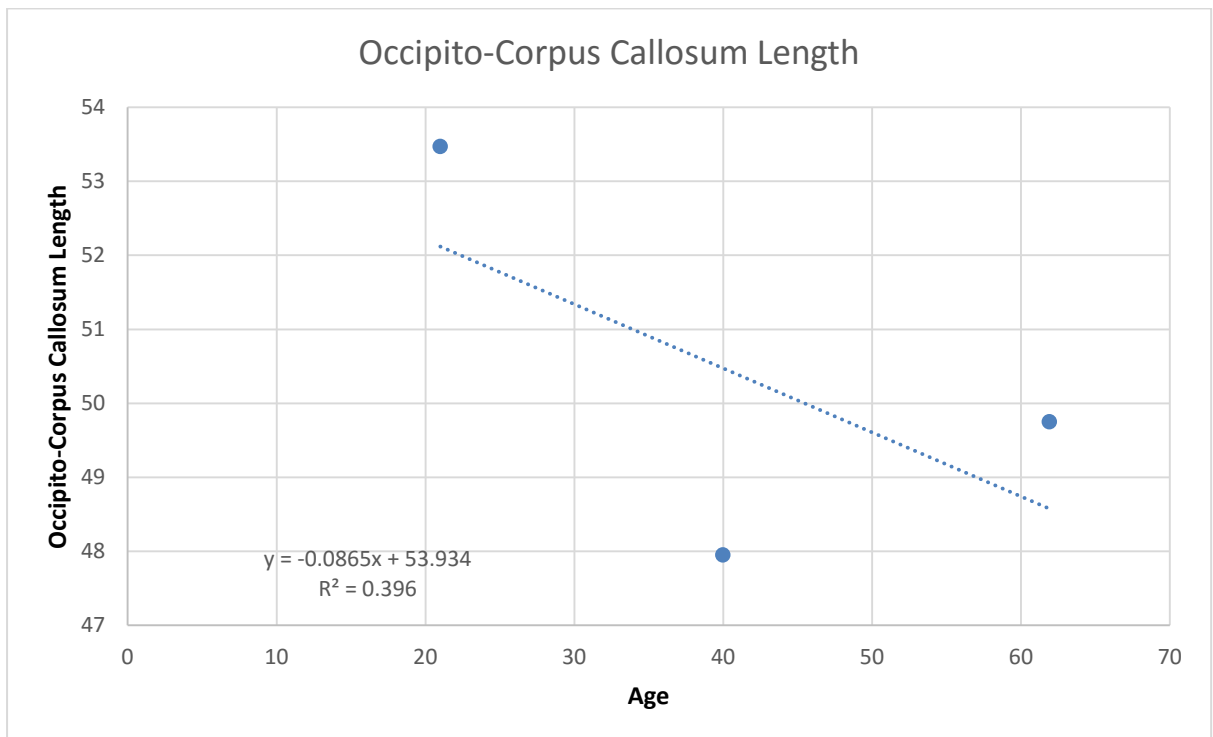


Figure 4.7 A scatter plot diagram shows a linear relationship between the **Occipito-Corpus Callosum Length** and the **Age** of the subjects, $R^2 = 0.396$.

Table 4.3 comparison between males and females:

Gender	Age (years)	Genu Width (mm)	Trunk Width (mm)	Splenium Width (mm)	Fronto-Occipital Length (mm)	Corpus Callosum Length (mm)	Fronto-Corpus Callosum Length (mm)	Occipito-Corpus Callosum Length (mm)
Male	35.6±18.4	11.4±1.6	6.2±1.1	11.3±2.1	162.7±7.7	75.0±6.0	36.8±3.0	52.4±5.7
Female	38.4±19.2	11.7±1.8	5.7±1.1	11.3±1.5	156.3±6.2	72.4±7.4	34.4±2.8	49.7±5.2

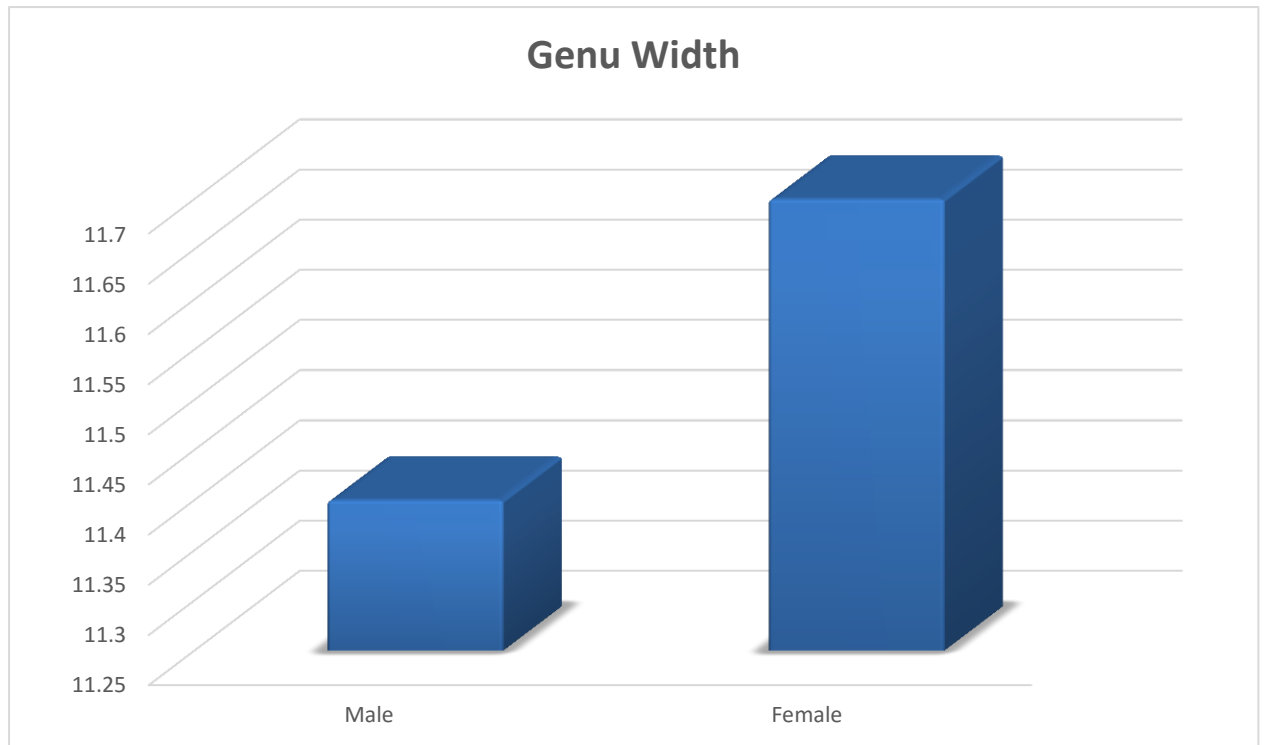


Fig 4.8: comparison between males and females in Genu Width

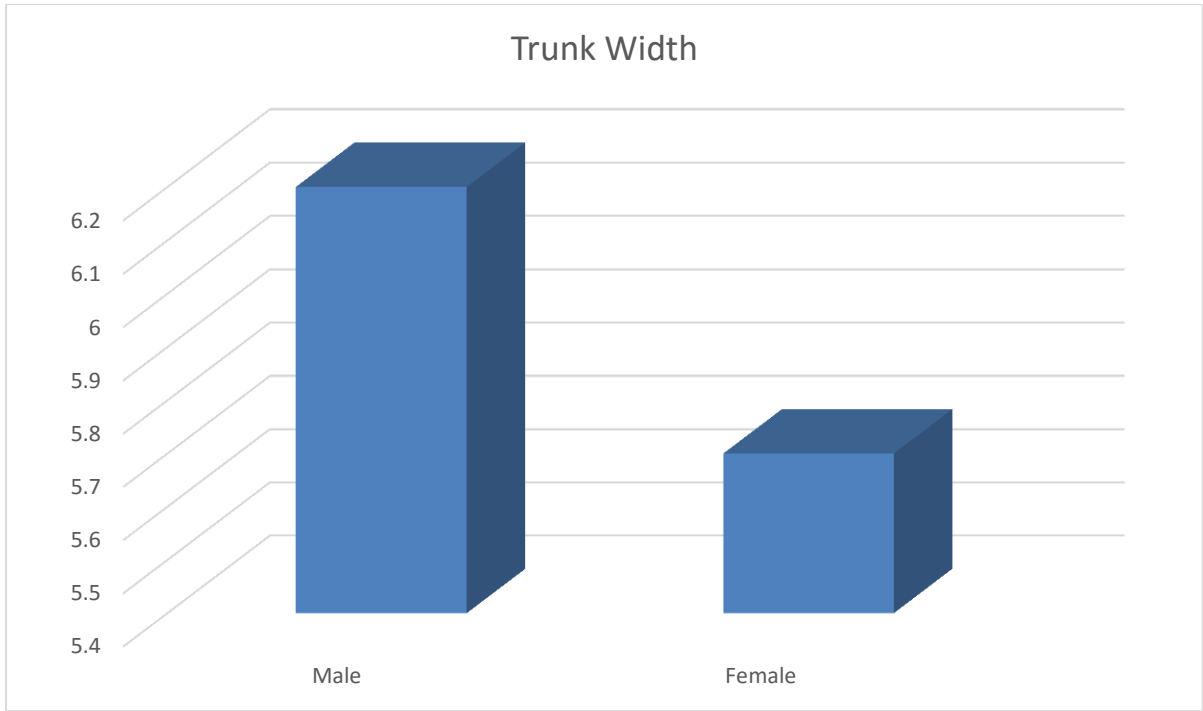


Fig 4.9: comparison between males and females in Trunk Width

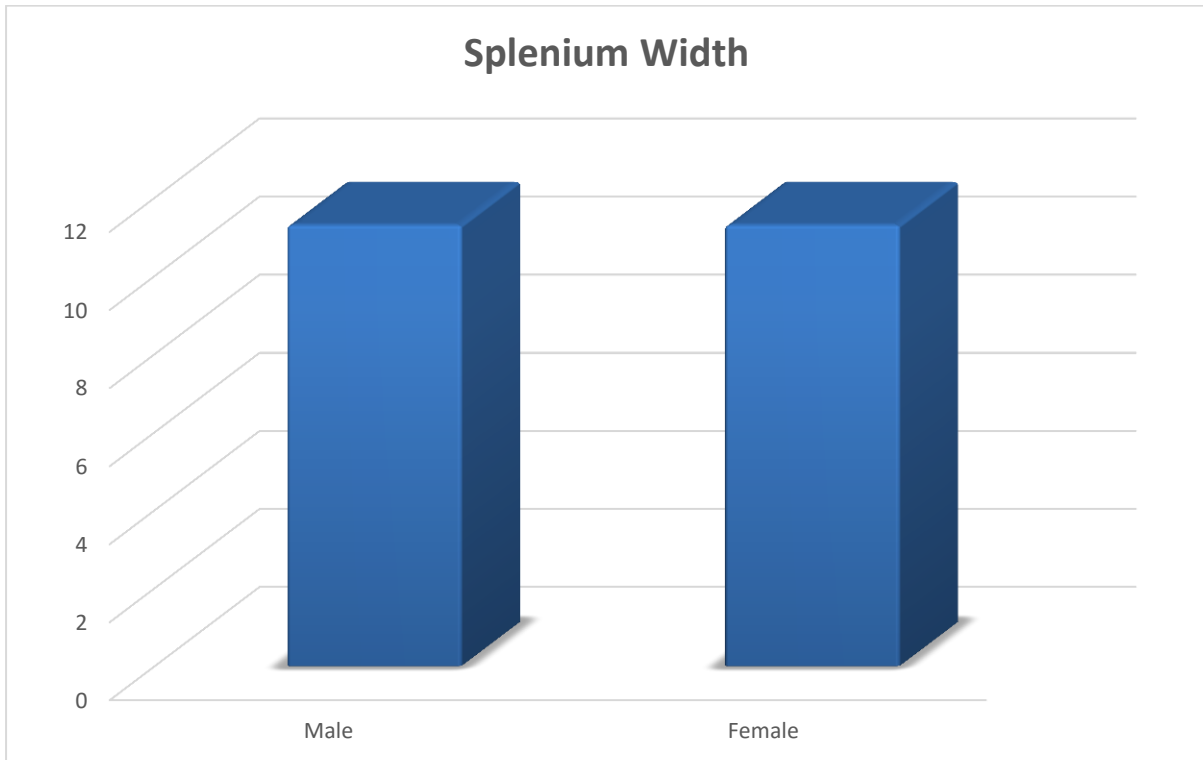


Fig 4.10: comparison between males and females in Splenium Width

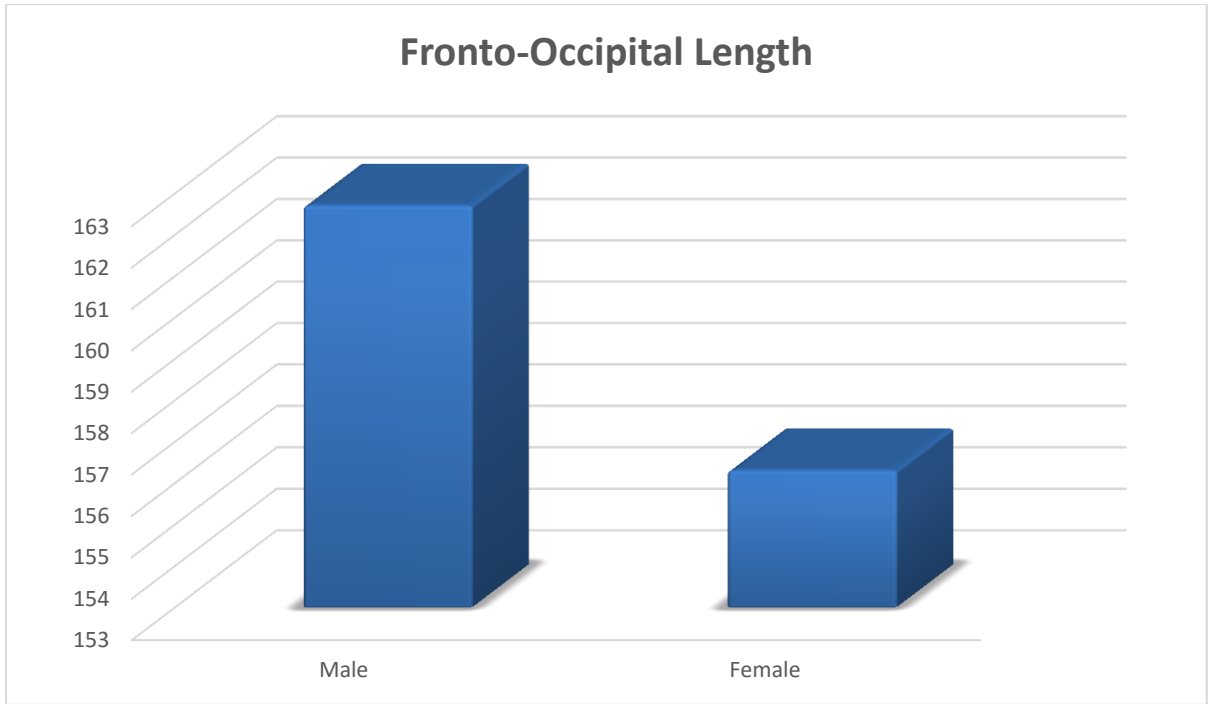


Fig 4.11: comparison between males and females in Fronto-Occipital Length

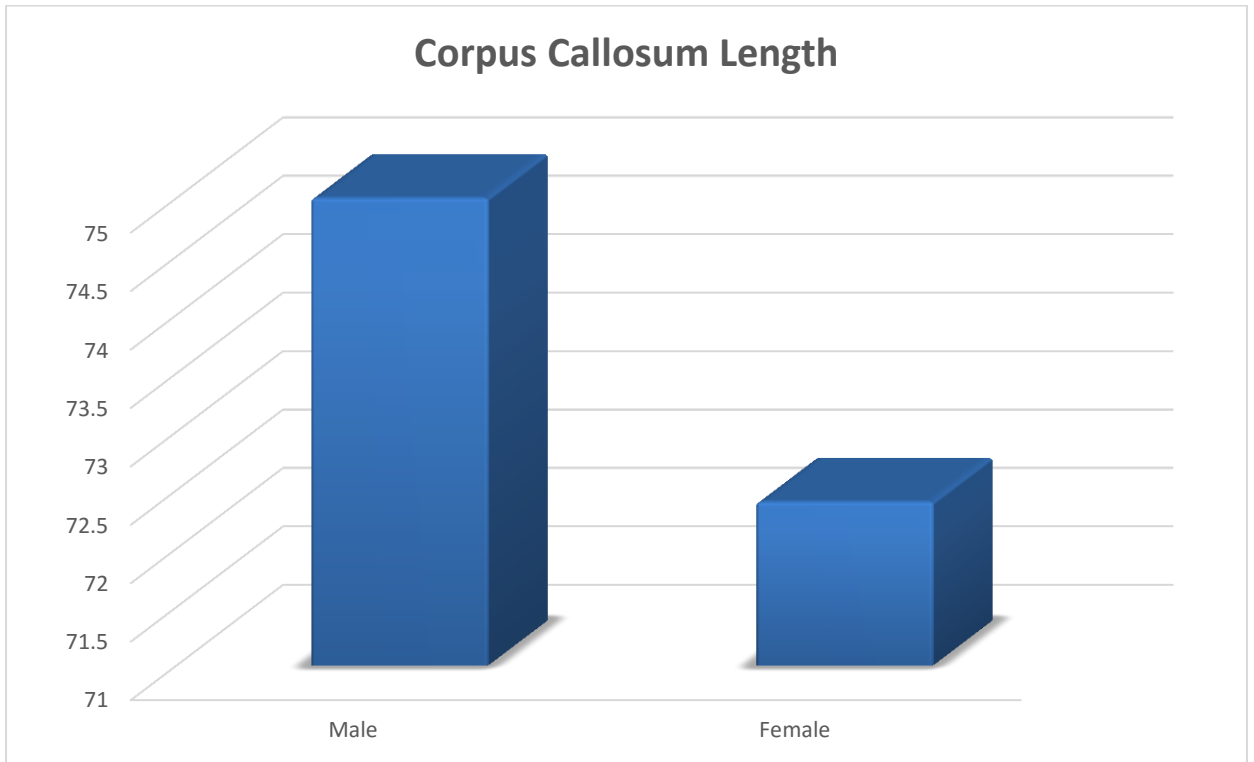


Fig 4.12: comparison between males and females in Corpus Callosum Length.

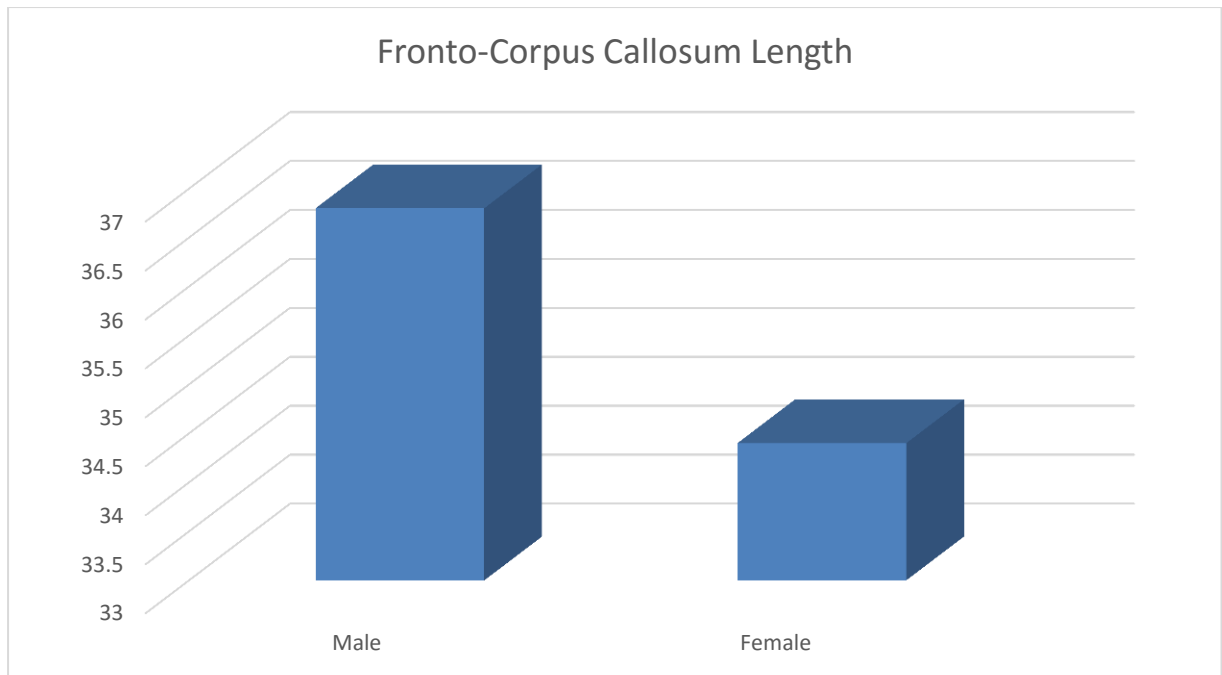


Fig 4.13: comparison between males and females in Fronto-Corpus Callosum Length.

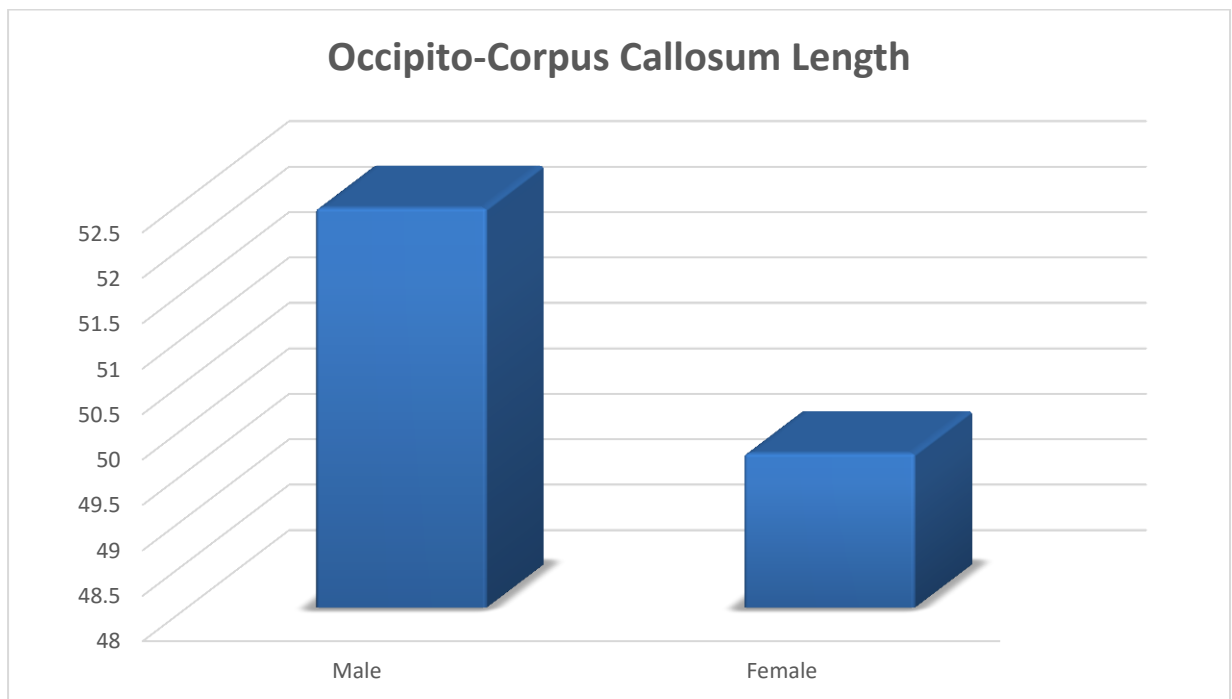


Fig 4.14: comparison between males and females in Occipito-Corpus Callosum Length.

Chapter Five

Discussion, Conclusion and Recommendations

5.1 Discussion:

The objective of this study was to characterize corpus callosum in normal Sudanese population using magnetic resonance imaging (MRI). This study was performed on 50 patients. The data collected from patients of ages ranged between 10-74 years old.

We found that the mean genu, trunk and splenium widths for total population were 11.63 +/- 1.77, 6.04 +/- 1.18 and 11.37 +/- 1.85 mm respectively. The corpus callosum length, fronto-occipital length, fronto-corpus callosum length, and occipito-corpus callosum length were 73.76 +/- 6.84, 159.59 +/- 1.85, 35.67 +/- 3.18 and 51.10 +/- 5.61 mm respectively (**Table 4.1**).

A significant negative correlation was observed between Genu Width and Age for total population ($r = -0.7277$) (**Fig 4.1**), A significant negative correlation was observed between Trunk Width and Age for total population ($r = -0.3951$) (**Fig 4.2**), A negative correlation was observed between Splenium Width and Age for total population ($r = -0.0008$) (**Fig 4.3**). A significant Positive correlation was observed between Corpus Callosum Length and Age for total population ($r = 0.082$) (**Fig 4.5**), Corpus Callosum increases in all its parts starting from 10 years until 50 years then start to decrease.

Males in comparison to females:

The mean age for females was 2.8 years higher than the mean age for males. The mean Genu width in females was higher than males by 0.3 mm (**Fig 4.8**), the mean value of the Splenium width was equal for both

males and females with increased standard deviation for males probably because of more diverse values for males (**Fig 4.10**), but the mean value of Trunk width, Fronto-Occipital length, Corpus Callosum length, Fronto-Corpus Callosum length, and Occipito-Corpus callosum length was higher in males than females by 0.5, 6.4, 2.6, 2.4, and 2.7 mm respectively (**table 4.3**) (**Fig 4.9, 4.11-14**).

These measurements were compared to study done by **Laissy J. et al** 2009, in Japanese population by MRI found the mean CC length for total population was 70.6 mm, which was higher than this study by 4.2 mm. Mean diameters for the genu, the body, and the splenium were respectively 9.6, 6, and 10.8 mm. which was more than this study by 2, 0.04, and 0.57 mm respectively This difference may be due to racial differences and patient habits.

Another study done by **Mohammadi MR et al.** in Turkish population by MRI found the mean value for the longitudinal dimension of the brain was 161.2 +/- 0.81 mm which was lower than this study by 1.6. The mean value for the longitudinal dimension of the CC was 70.6 +/- 0.52 mm, which was higher than this study by 4.2 mm. The mean value for the longitudinal dimension of the genu and the splenium was 23.5 +/- 0.17 mm and 14.1 +/- 0.10 mm respectively which was lower than this study by 11.9 and 2.7 mm respectively. This difference may be due to smaller sample size in this study, racial differences and patient habits.

5.2 Conclusion:

We concluded that According to the normal cells adaptation the age have direct effect on the corpus callosum size and noted that increase age lead to decrease corpus callosum, also the size of the corpus callosum is higher in male than female.

5.3 Recommendations:

Further study in evaluation of corpus callosum with larger sample of Sudanese population for more accurate results is needed.

Future studies should calculate the Corpus Callosum volume to give full demographic information.

References:

Arkovich AJ. (1996). Analyzing the corpus cal-losum. *AJNR Am J Neuroradiol*; **17**:1643–1645.

Catherine Westbrook (2008), Handbook of MRI technique, Blackwell Publishing Ltd, 3rd Ed.

Elster AD, Dipersio DA, Moody DM (1990) Sexual dimorphism of the human corpus callosum studied by magnetic resonance imaging: fact, fallacy and statistical confidence. *Brain Dev*; **12**: 321-5.

Hallak et al. (2007) Total Agenesis of the Corpus Callosum in a Patient with Childhood-Onset Schizophrenia, *Arq Neuropsiquiatr*; **65**(4-B):1216-1219

Herlidou-Même S et al (2003) MRI texture analysis on texture test objects, normal brain and intracranial tumors. *Magnetic Resonance Imaging*, **21**(9):989-93.

M.R.E Dean (1990) Basic Anatomy and Physiology for Radiographers, F.A. Davis Co., 1st Ed.

Mohammadi MR, Zhand P Moghadam BM, Golalipour MJ (2011) Measurement of the corpus callosum using magnetic resonance imaging in the north of iran. *Iran J Radiol*.**8**(4):218-223.

Mourgela S et al (2006) An MRI study of sex- and age-related differences in the dimensions of the corpus callosum and brain. *Neuroanatomy***6**: 63–65

Oliveira MS et al (2012) MRI-texture analysis of corpus callosum, thalamus, putamen, and caudate in Machado-Joseph disease. *JNeuroimaging***22**(1):46-52.

Standring S. et al.(2005) Gray's Anatomy: The Anatomical Basis of Clinical Practice (39ed). London Elsevier Churchill Livingstone 411-414.

Vishram Singh (2004), Textbook of Clinical Neuroanatomy, ELSEVIER, 1st Ed.

Appendices

Data Collection Sheet:

no	Gender	AB (Fronto-occipital length)	EZ (Cospus Callosum Length)	AE (Fronto-corpus length)	ZB (occpito-corpus length)	Age	Genu width	Trunk width	Splenium width	ZB (occpito-corpus length)

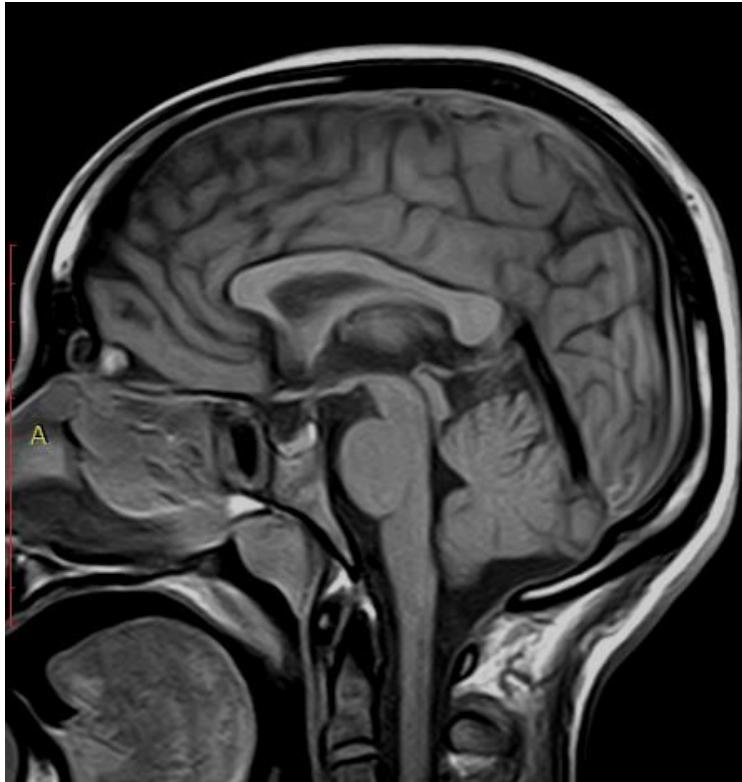


Fig 5.1: Sagittal T1 for male patient (40 Y) (TR: 676.0, TE: 10.0, slice thickness: 5.0 mm).

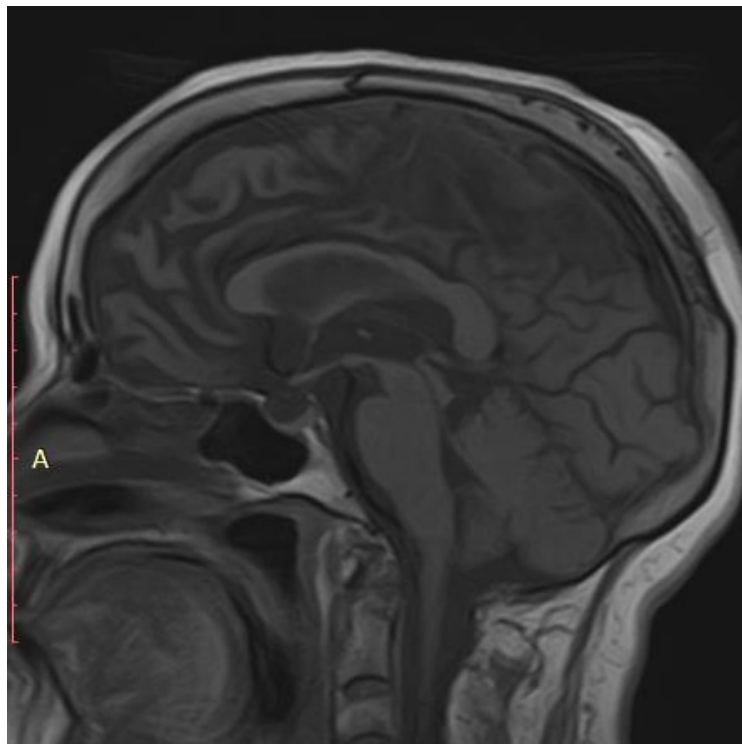


Fig 5.2: Sagittal T1 for male patient (55 Y) (TR: 676.0, TE: 10.0, slice thickness: 4.7 mm).

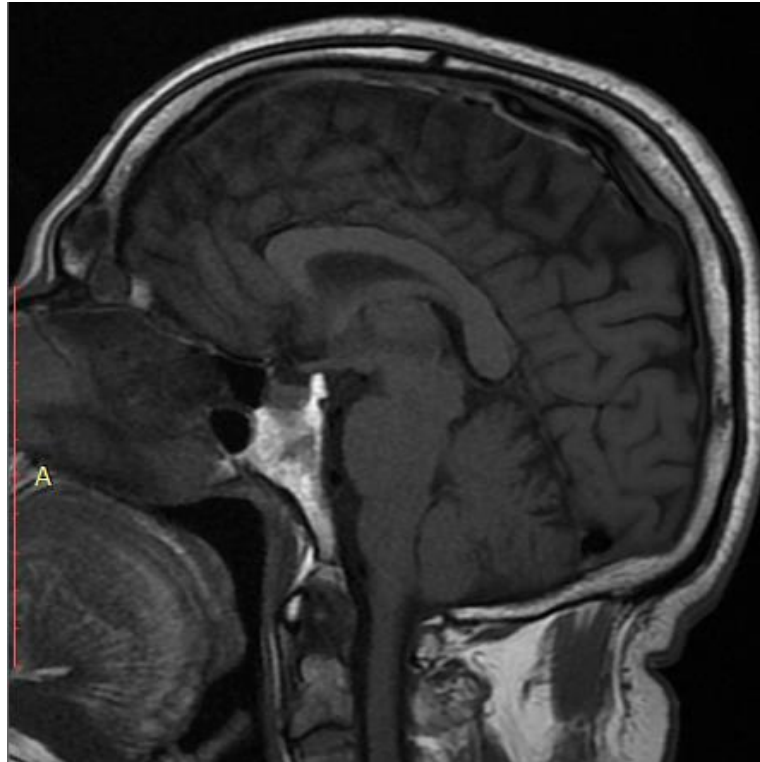


Fig 5.3: Sagittal T1 for male patient (60 Y) (TR: 676.0, TE: 10.0, slice thickness: 5.0 mm).

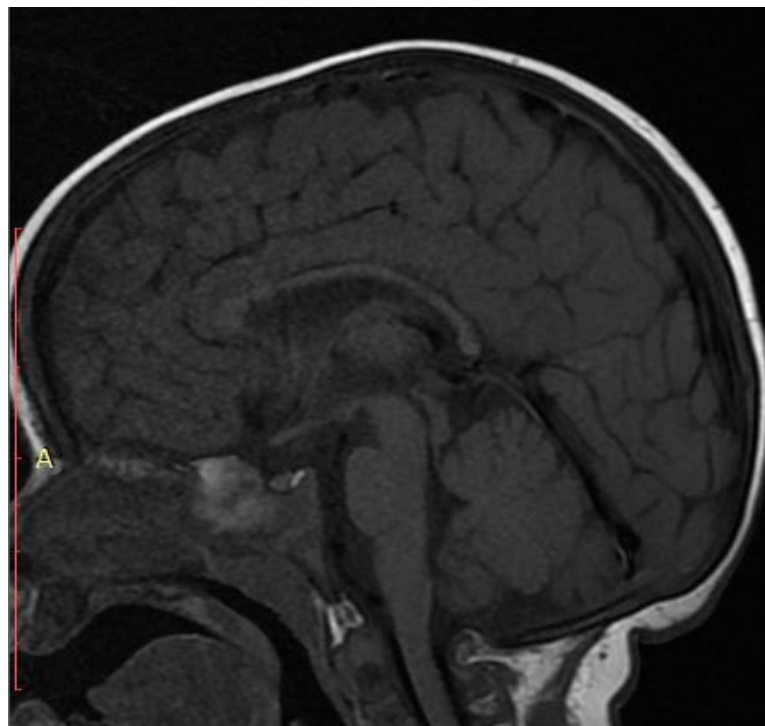


Fig 5.4: Sagittal T1 for male patient (10 Y) (TR: 676.0, TE: 10.0, slice thickness: 5.0 mm).

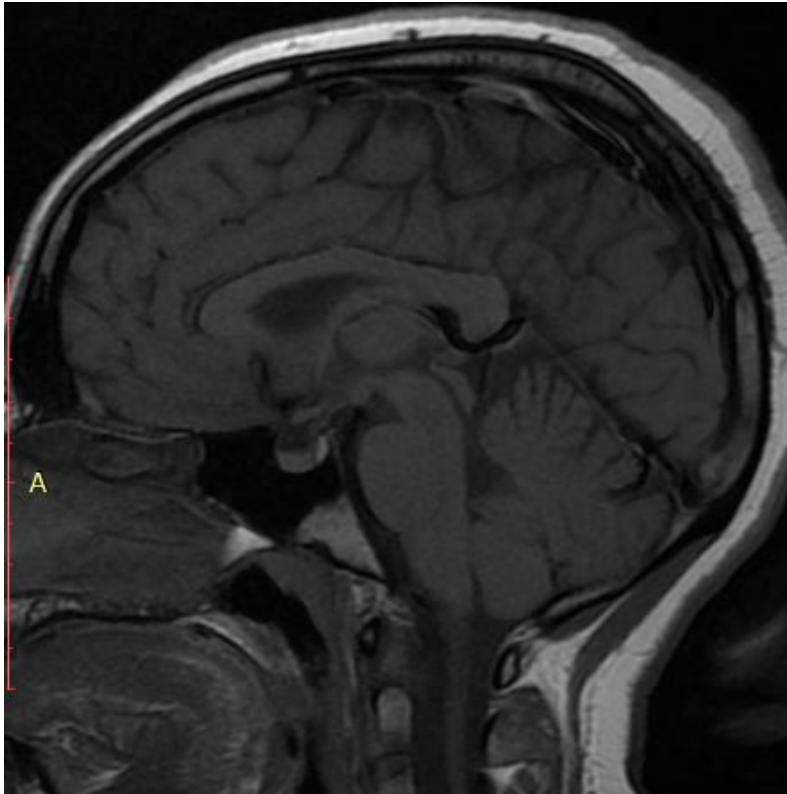


Fig 5.5: Sagittal T1 for female patient (23 Y) (TR: 676.0, TE: 10.0, slice thickness: 5.0 mm).

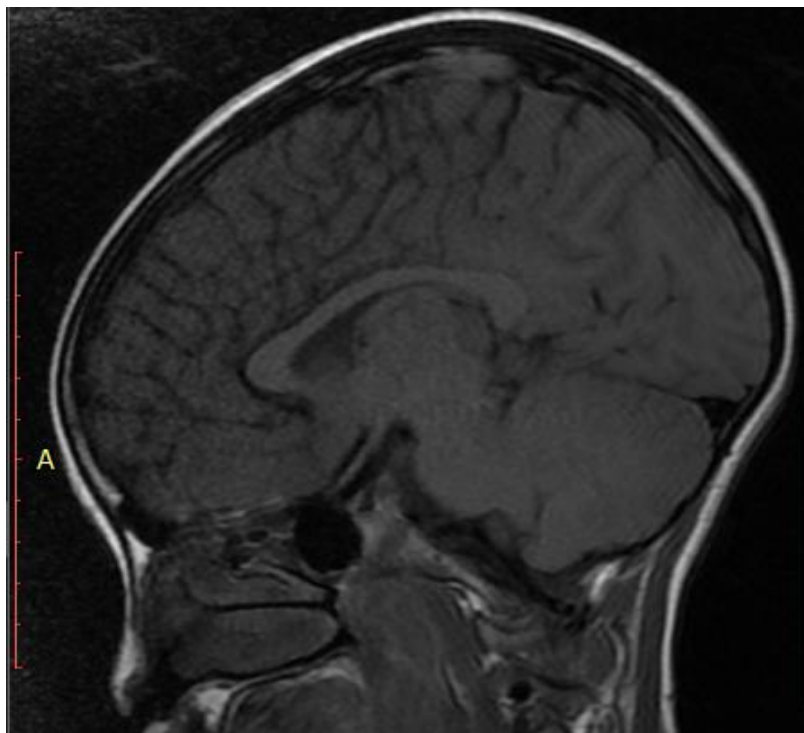


Fig 5.6: Sagittal T1 for female patient (12 Y) (TR: 676.0, TE: 10.0, slice thickness: 5.0 mm).

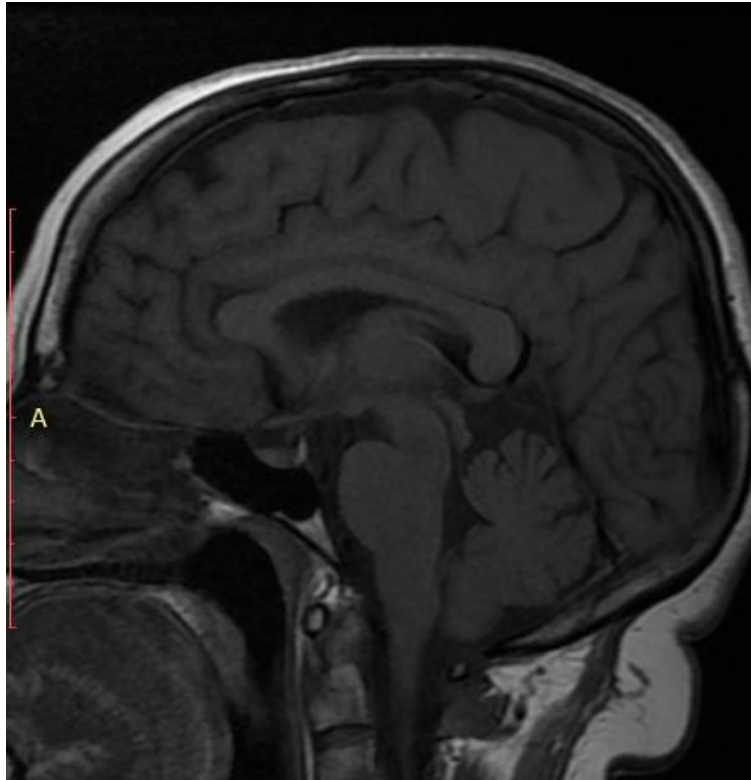


Fig 5.7: Sagittal T1 for female patient (50Y) (TR: 676.0, TE: 10.0, slice thickness: 5.0 mm).

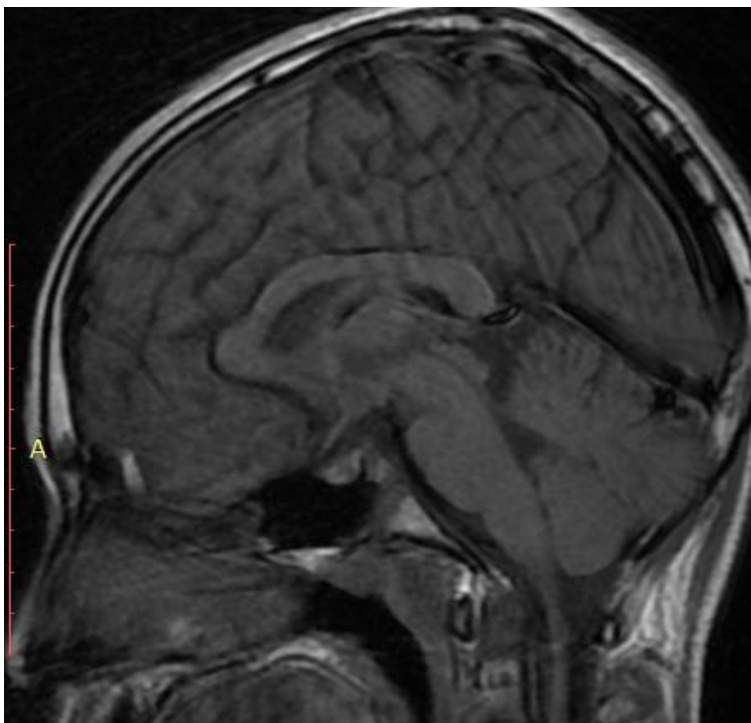


Fig 5.8: Sagittal T1 for male patient (20 Y) (TR: 676.0, TE: 10.0, slice thickness: 5.0 mm).

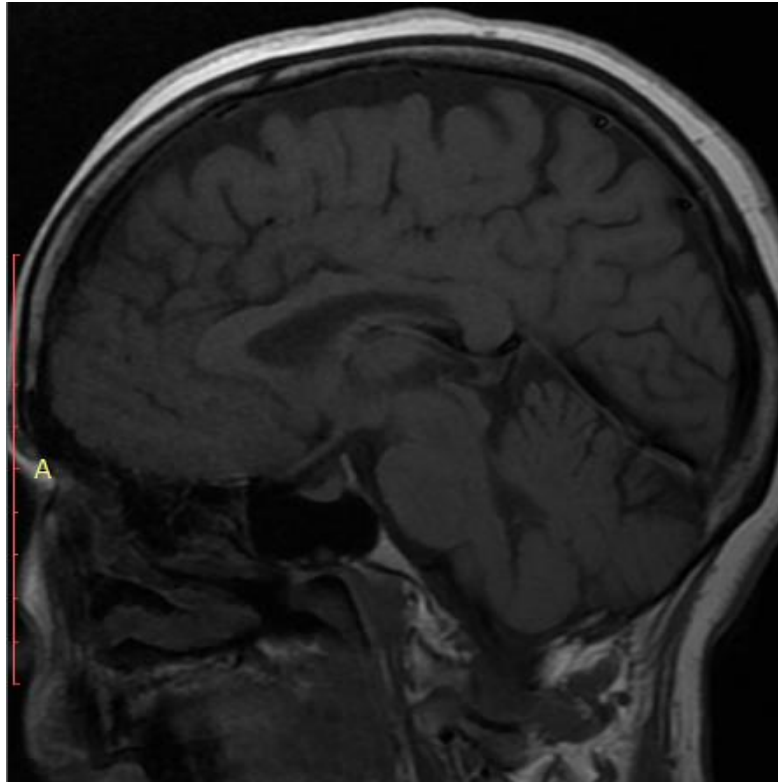


Fig 5.9: Sagittal T1 for female patient (45Y) (TR: 676.0, TE: 10.0, slice thickness: 5.0 mm).

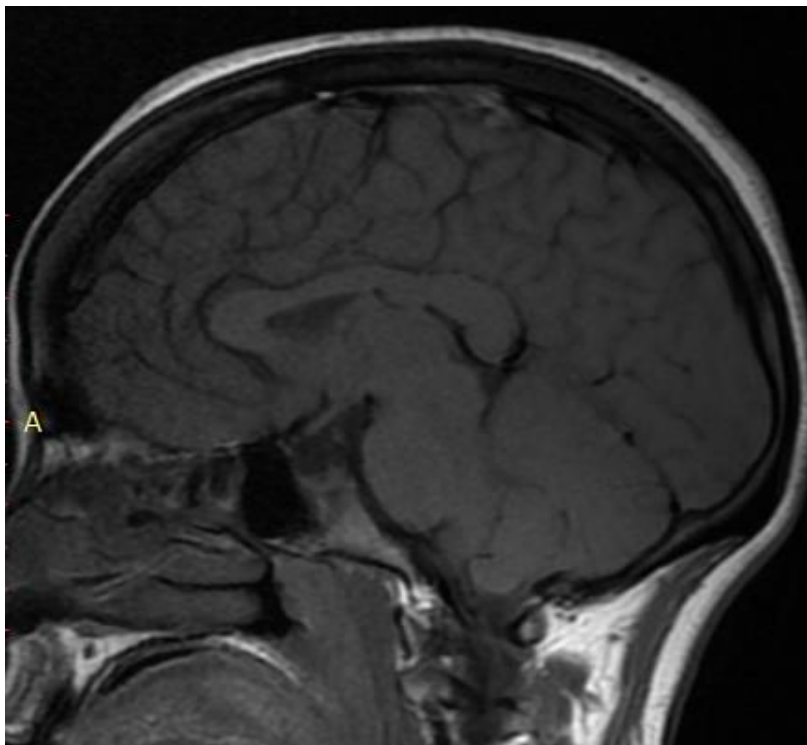


Fig 5.10: Sagittal T1 for female patient (25Y) (TR: 676.0, TE: 10.0, slice thickness: 5.0 mm).